University of Stavanger

Faculty of Science and Technology

MASTER'S THESIS

Study program/Specialization: Petroleum Geosciences Engineering	Spring semester, 2015 Confidential
Writer: Anastasia Titova	(Writer's signature)
Faculty supervisor: Karl Audun Lehne External supervisor(s): Chisom-Christiana Onubogu (TOTAL E&P Norge)	
Title of thesis: Electrofacies Analysis - A possible use in Paleogeographic understanding of a North Sea reservoir.	
Credits (ECTS): 30	
Keywords: Electrofacies Northern North Sea Paleogeography Correlation Logs Cook Formation	Pages: 70 +CD Stavanger, June 2015

Electrofacies Analysis -
A possible use in Paleogeographic understanding of
a North Sea reservoir.

by

Anastasia Titova

Master Thesis

Presented to the Faculty of Science and Technology

The University of Stavanger

The University of Stavanger

June, 2015

Acknowledgements

This master thesis is submitted as a partial fulfillment of the Master Degree of Science in Petroleum Geoscience Engineering. The research has been performed mainly in Total E&P Norge office, Stavanger during the spring term 2015.

I owe my thanks to Total E&P Norge, who provides me all the necessary data needed for the project, and the best work environment.

I want to dedicate my deepest gratitude to my supervisors, Chisom-Christiana Onubogu for defining this thesis project, keeping it for me as the most interesting project I have ever experienced, and for continuous support in software solutions; and to Karl Audun Lehne, for his great academic and personal support. I appreciate their patience, sharing of the knowledge, and guidance.

I also want to show my gratitude to the staff in Total E&P Norge for their professional help and personal advises during the project, particularly to Ole-Peter Hansen, Denis Francois, German Camargo, Marie-Lovise Valdresbraten, Patrick Martinet, Romain Bibonne and Dominique Roy. I am thankful to Philippe Rabiller for his recommendations and support.

The master thesis as part of my Master's Degree would not be possible without financial support from University of Stavanger Scholarship Scheme. I am highly grateful for the provided opportunity and experience, and especially to Associate Professor Nestor Cardozo and Professor Alejandro Escalona.

Last but not least, I feel much appreciated for my families and friends. Their belief gives me confidence and courage to accomplish my study and manage all difficulties.

Abstract

Electrofacies Analysis - A possible use in Paleogeographic understanding of a North Sea reservoir.

Anastasia Titova, MSc Degree in Petroleum Geoscience Engineering,

The University of Stavanger, 2015

Supervisors: Chisom-Christiana Onubogu (Total E&P Norge)

Karl Audun Lehne (University of Stavanger)

The study area is centered around the B prospect, which is situated in block 34/6, in the northern part of the Tampen Spur area, northern North Sea. In the study area, lateral changes in reservoir properties of the Lower Jurassic Cook Formation have been observed as well as the need to understand the overall trend and lateral continuity of the lithology within the depositional environments. Understanding of the paleogeography is crucial for prediction and evaluation of the reservoir qualities. Electrofacies could be a possible tool for reconstructing paleogeographic settings.

The study is based on eight wells drilled on the Cook formation, using basic log data as input (Gamma Ray, Density, Neutron Porosity Logs), and as additional logs like Sonic, Deep Induction and the Density-Neutron Separation computation. Existing petrophysical interpretation is also incorporated, together with information from cores and sedimentological analysis, to link electrofacies associations with depositional environment. The final electrofacies model is then propagated in wells without core data as well as in areas lacking detailed sedimentological analysis.

The results are used to understand the paleogeographic distribution of the identified lithofacies from one well to another in the area of interest and its possible implication in terms of:

- reservoir presence and facies typing,
- formation and layer tops correlation
- lateral variation and regional continuity.

Finally, this study can be used for possible future well locations.

Table of Contents

GLOSSARY

- GR – Gamma Ray Log
- RHOB or Dens – Density log
- NP or NEUT – Neutron Porosity Log
- DNS – Density Neutron Separation (represents porosity difference between RHOB and NP)
- PHIT – Total Porosity from petrophysical evaluation
- RT or RDEEP – Resistivity Log (also RDEEP or ILD – Induction Log)
- DT or SON – Sonic Log
- EF – electrofacies
- TEPN – Total E&P Norge
- HC – Hydrocarbon(s)
- Fm. – Formation
- Blind Test – Quality control of the final electrofacies model

List of Tables

List of Figures

1 INTRODUCTION

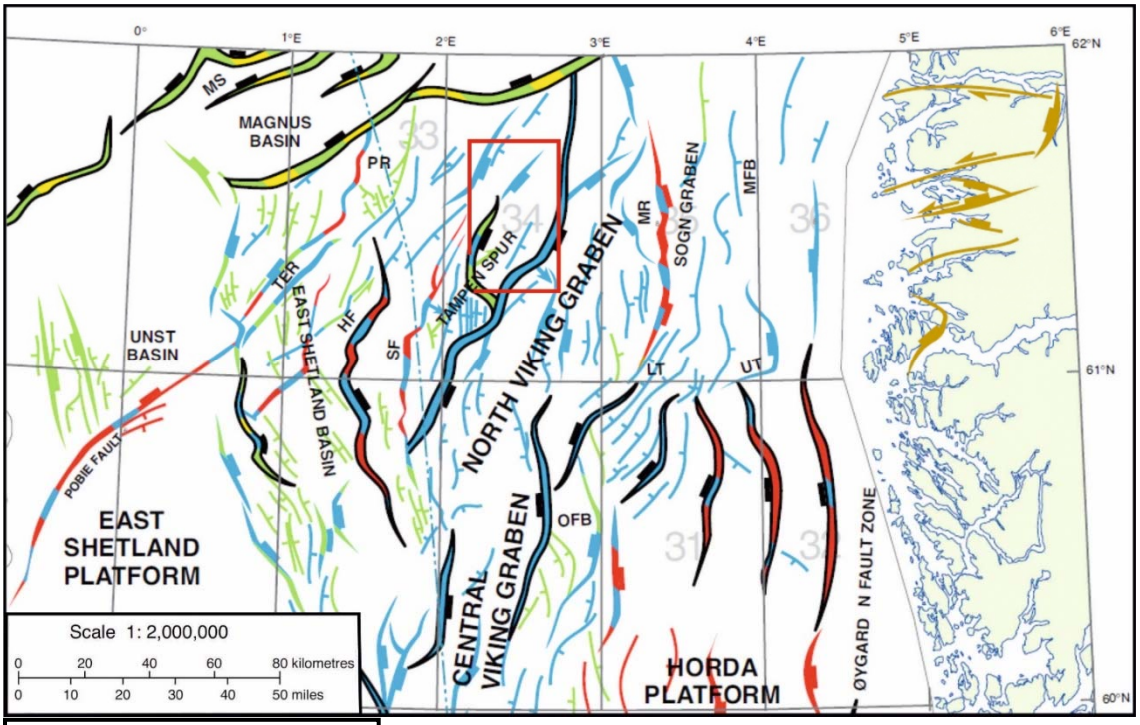

Figure 1: Location of the study area and structural framework (Modified after Evans et al., 2003)

The study area is centered around the B prospect, which is located in the northern North Sea and was found in 2012 (Figure 1). It is situated in block 34/6, in the northern part of the Tampen Spur area (Total Exploration and Production Norge AS (TEPN) – Well B1 Confidential Report, 2014).

The main reservoir target of the B prospect is the sandstones of the Lower Jurassic Cook Formation, which belongs to the Dunlin Group. The Dunlin Group is subdivided from base to top into Amundsen, Johansen, Burton, Cook, and Drake formations

(Volleset and Dore, 1984) and ranges from Hettangian to Bajocian age (Lithostatigraphy: Dunling Group, NPD FactPages).

The Cook formation is the primary hydrocarbon bearing reservoir in the study area (Norsk HYDRO – Final Well Confidential Report, 1992; TEPN – Well A1 Confidential Report, 2003), Knarr Field (Field: Knarr Field, NPD FactPages), and Blåbær discoveries (TEPN – Confidential Geological End of Well Report, 2010), while it is the secondary reservoir in the Statfjord and Veslefrikk fields (Marjanac and Steel, 1997), Gulfaks (Dreyer and Wiig, 1995), Oseberg (Livbjerg and Mjos, 1989), and the Kvitebjørn Fields (Folkestad et al., 2012). Deegan and Scull (1977) named the Cook Formation and gave it "sub-unit" status. Vollset and Doré (1984) renamed it and has since then been referred to as a formation rather than a sub-unit. The formation is laterally extensive distributed in the northern North Sea, and has been penetrated by more than 200 wells. Its thickness ranges from 40 to 120 m.

On the regional scale, the reservoir quality of the Cook Formation varies from East to West related to the distance from the clastic source area. In addition, local variations in the reservoir quality can be seen, linked to both primary depositional facies and secondary diagenetic facies (TEPN – Well B1 Confidential Report, 2014).

Most of the Cook sediments consist of tidal deposits, with sands deposited as either bars or channels. In addition, wave dominated shoreface sands are found within the Cook Formation (TEPN – Well B1 Confidential Report, 2014).

There appears to be a link between the reservoir quality and the sedimentary facies through textural petrographic characteristics. The best reservoirs are the medium-grained well sorted deposits, which are found in the foreshore, the lower part of distributary channel fills and the tidal bar topsets (TEPN – Well B1 Confidential Report, 2014). Some of the samples have chlorite coating that preserves primary porosity.

The fairly complex reservoir architecture of the Cook Formation reservoir of the B discovery is the main challenge. The complexity is a result of the amalgamation of a large number of anisotropic individual sand bodies of limited size. Additional problem arise due to the presence of possible barriers and baffles that also decrease reservoir quality (TEPN – Well B1 Confidential Report, 2014).

The reservoir complexity and challenges in reservoir characterization are related to several factors such as eustatic changes in sea level, accommodation space, diagenesis, and compaction. Therefore, understanding the paleogeography of the North Sea reservoir and its primary facies is a significant element for future exploration. It will also help to predict reservoir presence, thickness, lateral extent, reservoir connectivity and vertical lithological barriers.

1.1 Objectives

This study aims at using Gamma Ray (GR), Density (RHOB), Neutron Porosity (NP), Density Neutron Separation (DNS) logs, as well as associated logs such as Sonic log (DT) and Deep Induction log (ILD) from eight wells, as inputs to define the electrofacies, which could be used as an additional element for paleogeographic reconstruction.

- First, electrofacies are identified on the key (cored) well, and then, these electrofacies are calibrated to core and sedimentological description of this well;
- An electrofacies model is built using the key well;
- The core-calibrated model is propagated to the other wells with limited or no core information;
- Finally, the obtained model can be utilized in the area of study for defining the paleogeography, if a consistent link between electrofacies associations and sedimentary environment is proved.

1.2 Previous works

1.2.1 COOK FORMATION

As the Dunlin Group became famous for its hydrocarbon bearing sands, depositional and tectonic settings, sequence stratigraphy, architecture of the Dunlin Group has been an active subject of study during 1990's to 2000's (Marjanac, 1995 ; Parkinson and Hines, 1995 ; Chamock et al., 2001 ; and Gibbons et al., 2003). When the Cook was discovered as a secondary reservoir in Statfjord, Gulfaks, and Oseberg Fields, studies on sequence stratigraphy, depositional environment, paleogeography and reservoir architecture and production analysis were implemented (Dreyer and Wiig, 1995; Marjanac, 1995; Parkinson and Hines, 1995; and Chamock et al., 2001). However, limited literature is published regarding electrofacies analysis of the Cook Formation.

One of the key studies carried out using electrofacies is that done by Gupta and Johnson in Gulfaks Field (2001). This study aims using electrofacies for recognition and distinction of the heterolithic deposits in the tide-dominated Lower Jurassic Cook Formation (Gupta and Johnson, 2001). Gupta and Johnson subdivide the Cook Formation into three units with a focus on the top most, Cook 3, being the primary target interval of this study, and this corresponds to the Upper Cook of the B discovery.

1.2.2 ELECTROFACIES ANALYSIS

Electrofacies "is a set of log responses that characterizes a sediment and permits the sediments to be distinguished from others". The term was first introduced by Serra and Abbott (1982, p. 118) and aimed connect log responses with geological attributes (Doveton, 1994). The method was popular in 1990's, however, later its usage became rare. Today, there is a renewed interest in the usage within the oil industry and is implemented for reservoir properties characterization, unconventional

resources studies, and reservoir volume estimation (Kumar and Mahendra , 2006; Stinco , 2006; and Teh , 2012).

1.3 Structural settings

The study area is situated at the boundary between the Tampen Spur (Figure 1) and the North Viking Graben (TEPN – Well A1 Confidential Report, 2003).

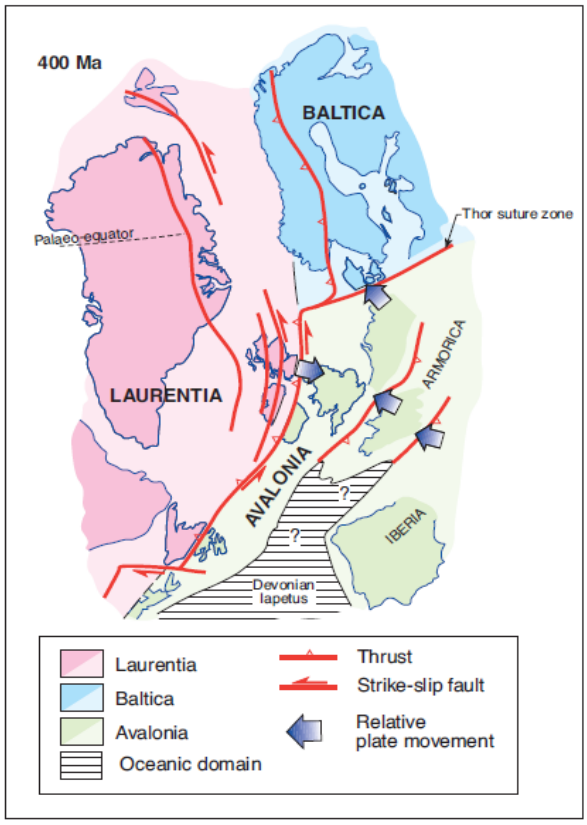

Figure 2: Evolution of the Caledonides (from Evans et al., 2003)

The basement of the North Sea consists of three Precambrian tectonic domains, namely, Avalonia, Laurentia, and Baltica (Figure 2), which collided during several stages of the Caledonian and Variscan orogenic events (Evans et al., 2003).

During the Mesozoic, the Tampen Spur area undergoes two main phases of rifting followed by subsequent post-rift subsidence in the Permian – Early Triassic and Middle Jurassic to Early Cretaceous (Evans et al., 2003; TEPN – C Field Confidential Report, 2013). The first rift stage reworks pre-existing Precambrian-Paleozoic accretionary structures (Evans et al., 2003) and produces a North-South trending fault system (Figure 1, Triassic faults on the legend), although notably having little effect to the study area (TEPN – C Field Confidential Report, 2013).

Following the initial rifting stage, between the Middle Triassic and the Middle Jurassic, the North Sea experiences post-rifting subsidence, which may have

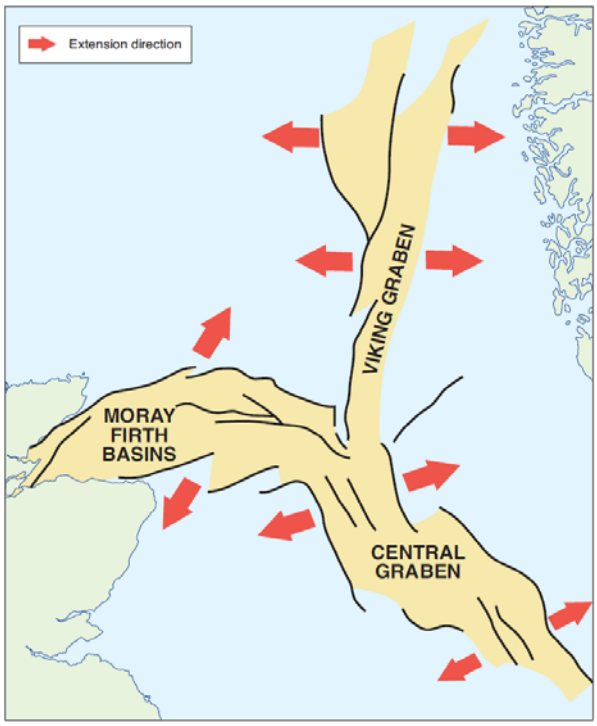

Figure 3: Triple-rift system generated in Mid-Jurassic to Early Cretaceous (Modified after Evans et al., 2003)

influenced the thickness distribution of the sediments (Chamock et al., 2001). Thus, Lower Jurassic Statfjord and Dunlin Groups are accumulated in mild tectonics conditions. Besides that, it is believed that during the Middle Jurassic, a mantle hot spot exists in the central North Sea and influences the accumulation of the important Brent Group reservoirs of the northern North Sea (Evans et al., 2003).

The next rifting phase took place from Mid-Jurassic to Early Cretaceous. Strong rifting processes affects the northern North Sea, producing a triple rift system (Figure 3) consisting of the Viking Graben, Central Graben, and Moray Firth Basins (Evans et al., 2003). In the study area, stretching reactivates the first stage faults and forms new normal faults. The newly formed blocks are rotated and experience upliftment such that their eastern edges undergo erosion.

By the Early Cretaceous, the structure of the B prospect is mostly established. Since then, the northern North Sea area continues to subside during the Cretaceous.

Finally, during the Late Cretaceous, tectonic inversion event gently deforms the North Sea Basin, and thereafter in the Cenozoic, the basin margins undergo major uplift (Evans et al., 2003).

In general, the pre-existing Triassic rift topography, deposited during stabilized tectonics under regional post-rift subsidence, has played a fundamental role

in defining the Lower Jurassic rock architecture. As a result, the elongated, westerly dipping three-way dip closure (Figure 4) associated to the tilted Jurassic fault block, which is bounded by east-facing normal faults, constitutes a structure of the B prospect. It is assumed that the Base Cretaceous Unconformity provides a trap at the crestal area in the east (TEPN – Well B1 Confidential Report, 2014).

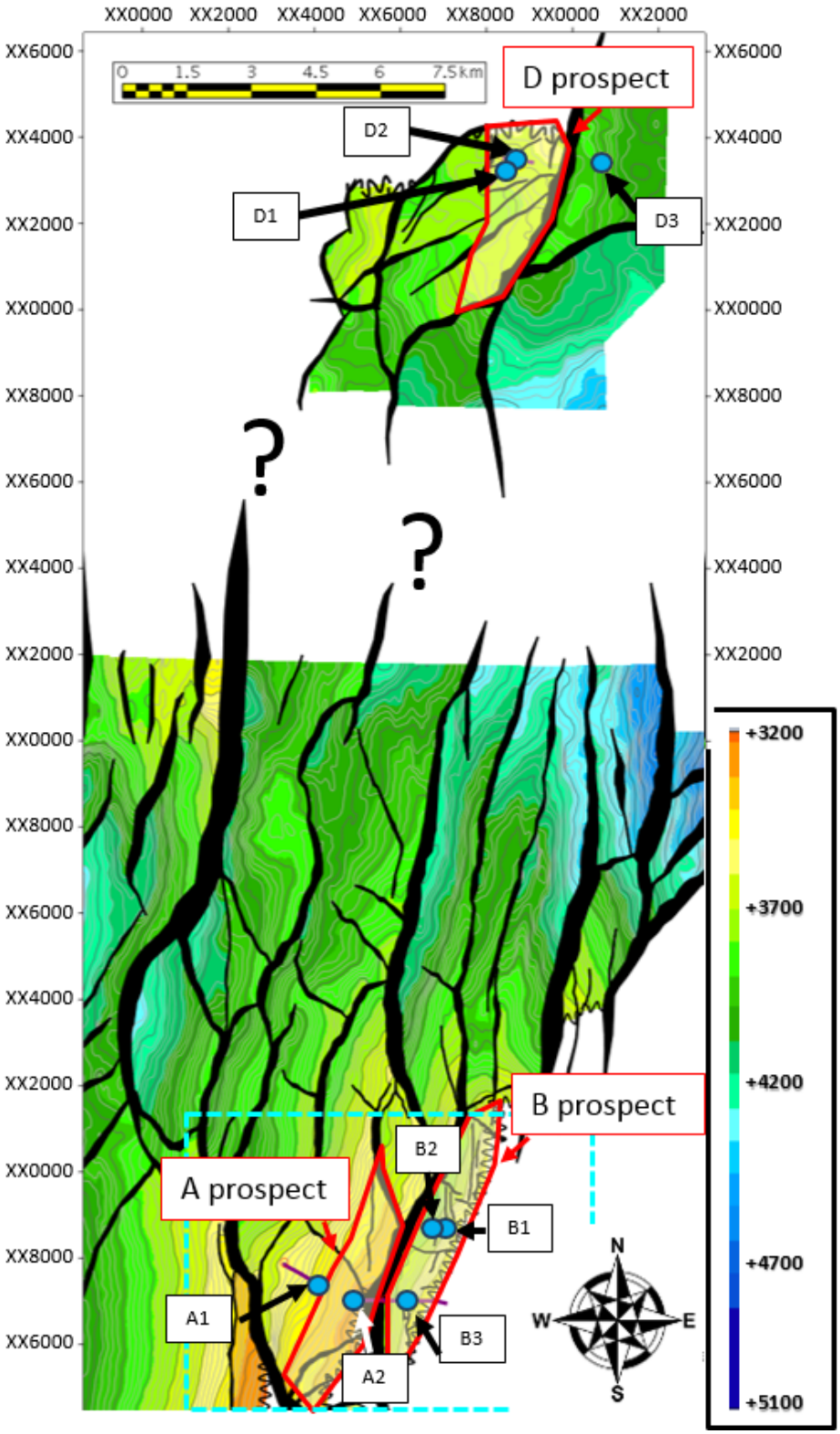

Figure 4: Top Cook structural map, showing the location of the main study area, displayed in blue dashed rectangular. Prospects A, B and D shown in red polygons with blue dots, representing the drilling location of the Top Cook Formation for each wells

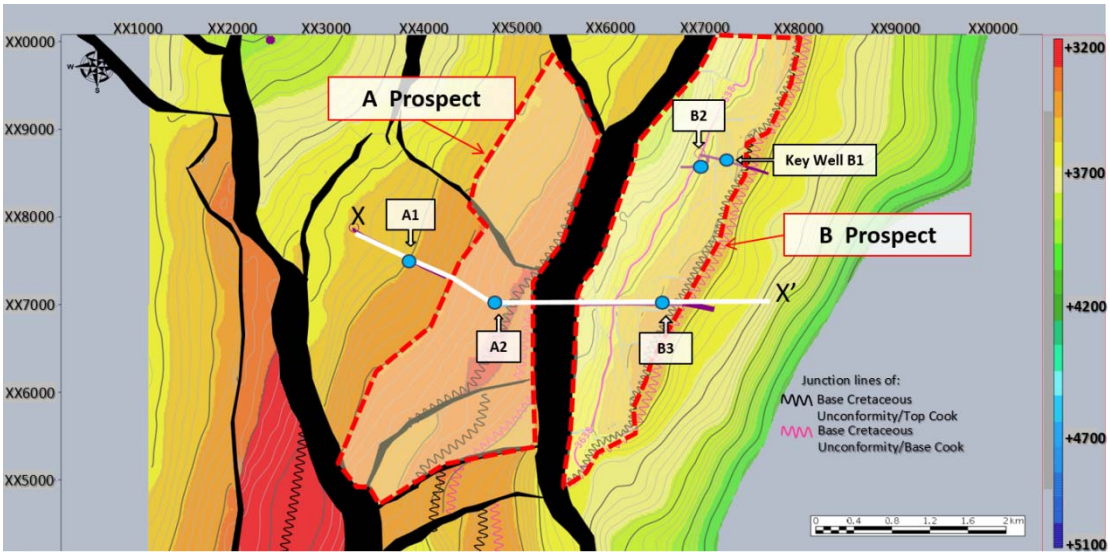

Figure 5: Composite Top Cook and Base Cretaceous Unconformity (BCU) structural map, showing A and B prospects (dashed red polygons) and wells, penetrated these prospects (blue points). White line is cross-section illustrated on Figure 6.

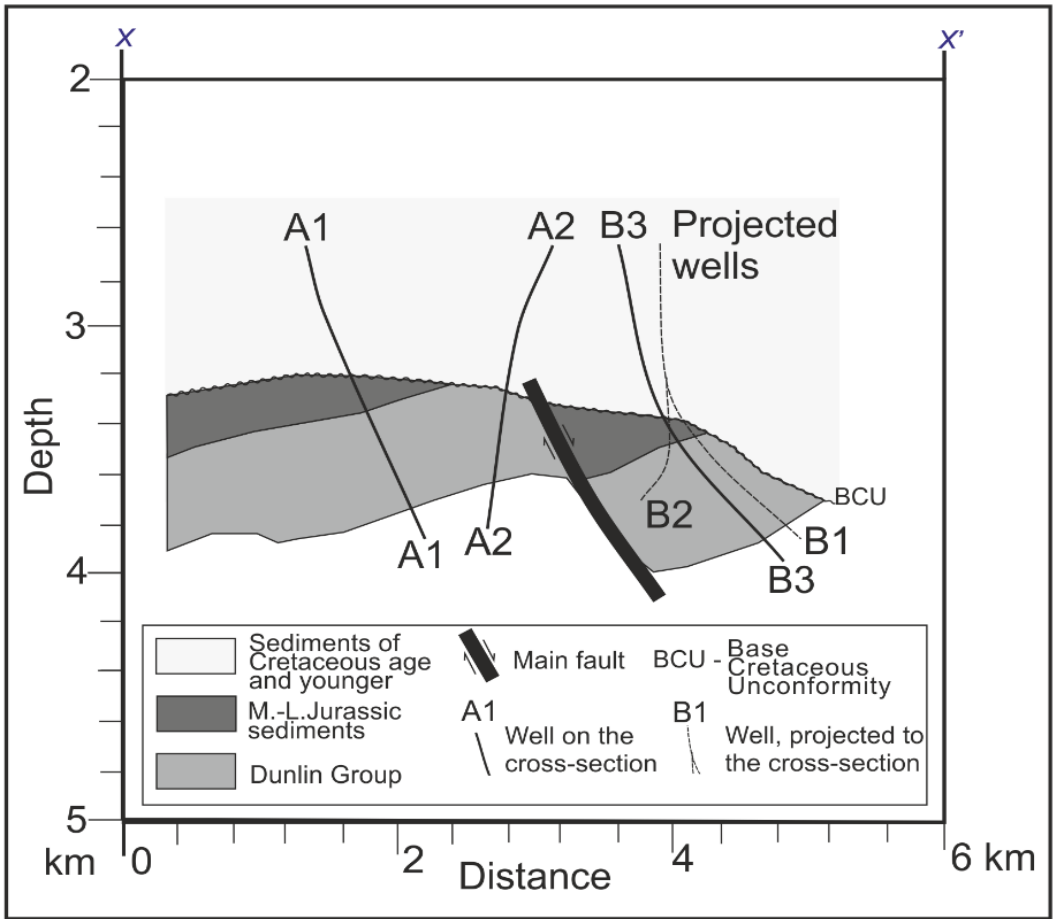

Figure 6: Schematic cross-section X-X' through prospects A and B (Modified after TEPN – Well B1 Confidential Report, 2014).

1.4 Stratigraphy

The northern North Sea is notable for a continuous Triassic–Jurassic succession. The particular interest of this thesis is Lower Jurassic Cook Formation of the widely distributed Dunlin Group (Figure 7).

The Dunlin Group comprises of shallow marine mudstones, siltstones, sandstones and locally distributed limestones (Parkinson and Hines, 1995, Lithostratigraphy: Dunling Group, NPD FactPages) sourced from the eastern Norwegian mainland (Evans et al., 2003). The Cook Formation consists of sandstones, siltstones and claystones with occasional calcareous doggers (Lithostratigraphy: Cook Formation, NPD FactPages; TEPN – Well A1 Confidential Report, 2003). The Cook sandstones correspond to a complex shallow marine and coastal system, including a variety of deltaic-, tide-,

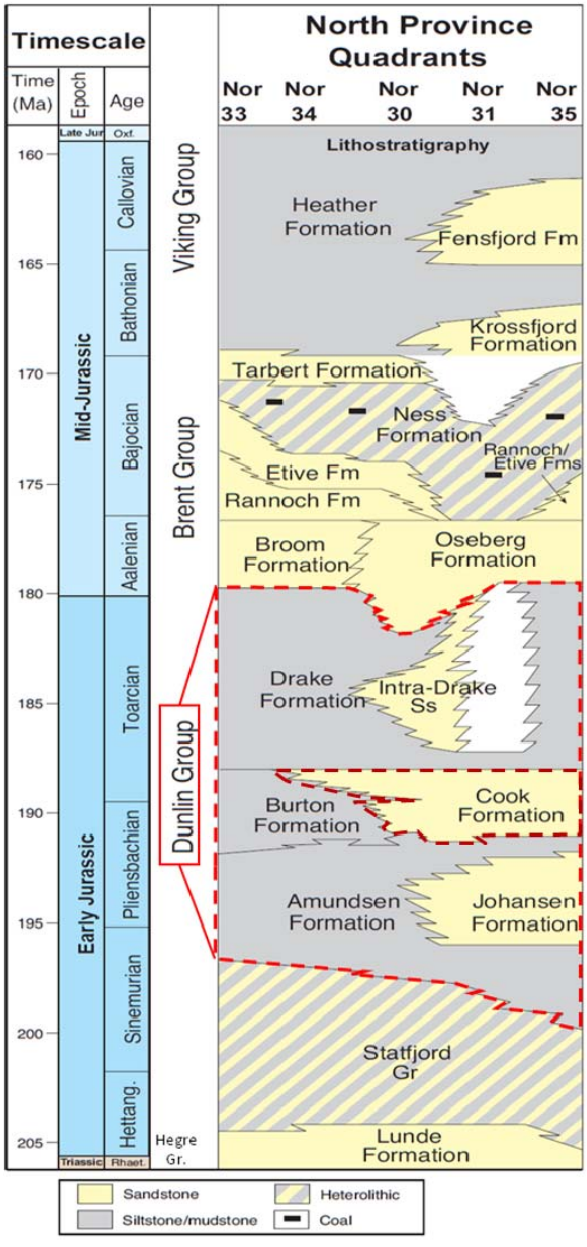

Figure 7: Lithostratigraphy of the study area (Modified after Evans et al., 2003)

estuarine and storm dominated sand bodies, with an overall westwards progradation trend (TEPN – Well B1 Confidential Report, 2014).

Recent internal TEPN studies (TEPN – Confidential Report, 2001) describes the boundaries of the Cook "Lithographic Unit" as diachronous, although the age is defined from Pliensbachian to Toarcian (Lithostratigraphy: Cook Formation, NPD FactPages). On the regional scale, the lower part of the Cook shales out into the Burton Formation, while in the upper part, a series of backstepping wedges shales out into the overlying Drake shale facies.

Many researchers identify two large scale cycles within Cook Formation; regressive cycle (lower) and transgressive cycle (upper), and this subdivision is valid for the B prospect area as well. The lower part is believed to be a prograding deltaic system, overlain by deposits of sandy delta front to lower delta plain with series of fluvio-tidal distributaries (TEPN – Well B1 Confidential Report, 2014). The Upper part depositional environment is interpreted as a mixed wave- and tide-dominated barrier-lagoon system in a non-deltaic context (TEPN – Well B1 Confidential Report, 2014). Based on the latest sedimentological and stratigraphic interpretations (Figure 8), seven reservoir layering is established at the scale of the B discovery structure and is being used as the current subdivision of the Cook Formation (TEPN-Well A1 Confidential Report, 2003).

Reservoir quality of the Cook sandstones varies both laterally and vertically within each field. The formation has been subdivided into 7 layers; (from bottom to top) layers 1-5 corresponds to the Lower Cook and layers 7-6 to the Upper Cook, shown on Figure 8.

Generally, reservoir properties of the Lower Cook are better than those of the Upper Cook. Reservoir quality of the Lower Cook is of good to moderate with porosity (Ø) generally ranging between 15 – 30% and permeability (K) of non-burrowed sandstones from 0,1 to 6D. Upper Cook layers consist of fine-grained sands

with Ø ranging between 12–17% and K from 0,06 to 2D. Mechanical compaction is the main cause of porosity loss in the reservoir sandstones. Calcite cemented zones are present in the Cook formation and more prominent in the Lower Cook (TEPN – Well B1 Confidential Report, 2014).

There are observed relationships between core facies and reservoir properties. Highly bioturbated facies that correspond to layers 6 and 7 have core Ø and K values of 10–15% and less than 0,001D respectively. The wavy and cross-bedded facies are heterogeneous sandstones that show good reservoir properties with core Ø ranging between 16-35% and K varying between 0,020-3D correspond to 1^{st} – 5^{th} layers on Figure 6. Several samples have abnormal good Ø and K, and these values are probably caused by effect of early chlorite coating (TEPN – Well B1 Confidential Report, 2014). In addition, as the grain size highly affects the reservoir properties, the best sandstones found are medium-grained, which are the most common for channel bases and tidal bars topsets.

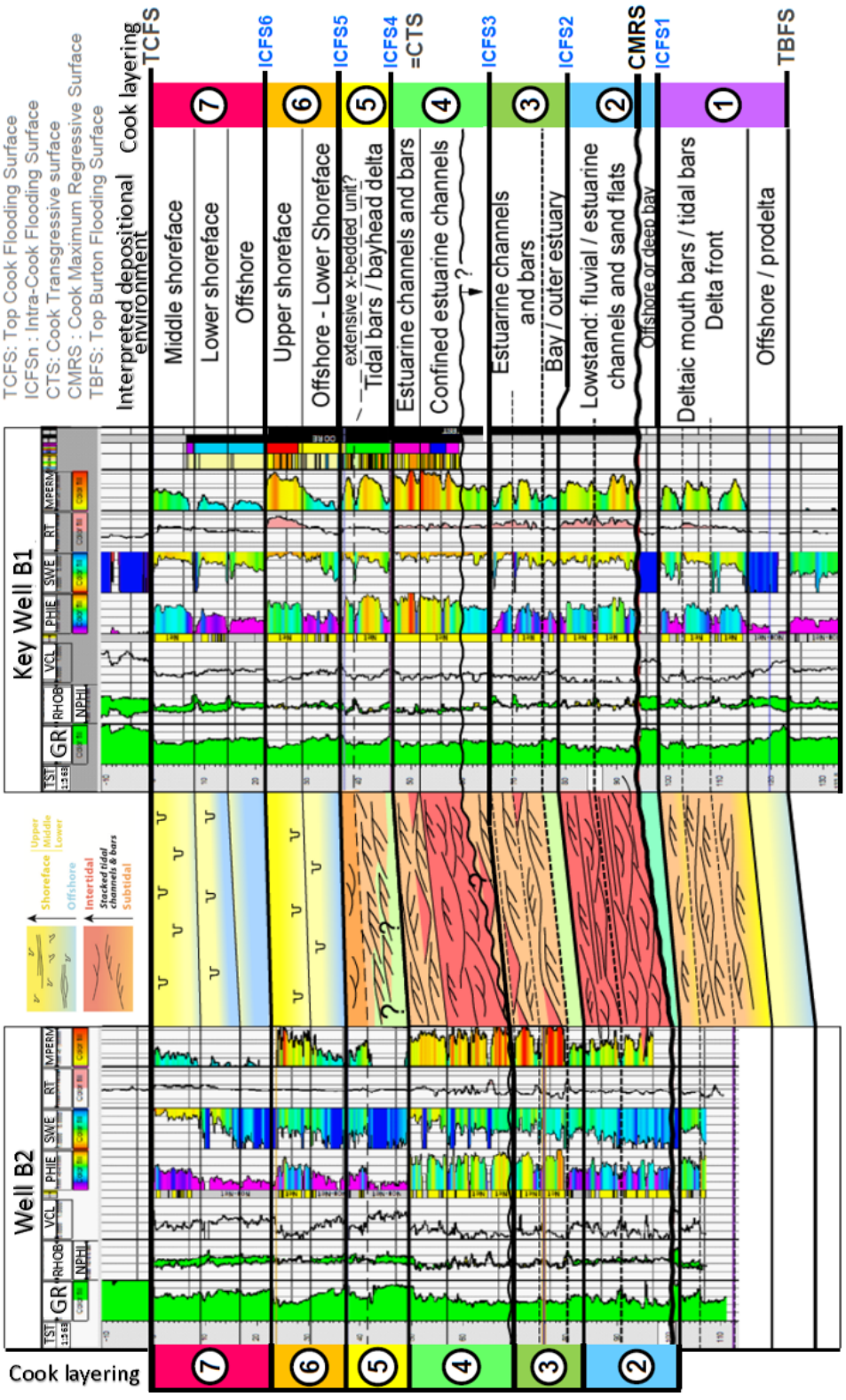

Figure 8: Stratigraphic layering basis of the B discovery geomodel (Modified after TEPN– Well B1 Internal Report, 2014)

2 METHODOLOGY AND DATASET

2.1 Dataset and Well Information

2.1.1 AVAILABLE DATA

In order to generate an electrofacies model that can be applied within the B-prospect and its environments, Total E&P Norge provided the dataset of conventional wireline logs as well as lithologs, final well and post well study reports, from eight wells, cores from four wells, sedimentary facies from two of the B-prospect wells, and image facies from one Well B3. The Table 1 shows summary of wells and the data available. This dataset together with reports from post mortem studies, internal presentation documents and reports from the Norwegian Petroleum Directorate (NPD) are additional sources of information used in this study

.

Table 1 Wells and available dataset

No of wells	Name	Prospect	GR	RT	NP	DT	RHOB	Core	PHIT log	Sedimentary Facies	Image Facies	Blind Test
1	A1	A	•	•	•	•	•		•			
2	A2		•	•	•	•	•		•			
3	**B1 Key well**	**B key study area**	•	•	•	•	•	•	•	•		
4	B2		•	•	•	•	•		•			
5	B3		•	•	•	•	•	•	•	•	•	•
6	D1	D	•	•	•	•	•	•	•			
7	D2		•	•	•	•	•		•			
8	D3		•	•	•	•	•	•	•			

Conventional wireline logs implicated in the Table 1 are the following:

- GR – Gamma Ray Log
- RHOB – Density log
- NP – Neutron Porosity Log

- DNS – Density Neutron Separation (represents porosity difference between RHOB and NP)
- PHIT – Total Porosity from petrophysical evaluation

In addition, the need for detailed study and better facies classification requires the use of Resistivity and Sonic Logs as associated logs:

- RT – Resistivity Log (also RDEEP or ILD – Induction Log)
- DT – Sonic Log

The available data covers most section in the wells drilled to the Total Depth (TD), but for the scope of study, the processing interval is limited to the key reservoir of interest (Cook Formation) as well as the shales directly above and below it that belongs to Drake and Amundsen Formations respectively (Table 2).

Table 2 Processing range for the study

No of wells	Name	Top	Bottom
1	A1	3580	4210
2	A2	3520	3960
3	B1	3600	3860
4	B2	3682	3954
5	B3	3760	4110
6	D1	3800	4130
7	D2	3932	4140
8	D3	3885	4300

2.1.2 WELL INFORMATION

Wells that belong to prospect B and A are main wells for this study, while wells from prospect D are provided in order to evaluate the possibility of the electrofacies model propagation on a regional scale (Figure 4).

2.1.2.1 Prospect A

Well A1 was drilled in 2002 and located in the west-central part of the A prospect (Figure 4-6). The well targeted Brent, Cook and Statfjord Formations, however, no significant shows were found (Wellbore: NPD FactPages). Well A2

penetrated prospect A in its east-central part in 2014, and is a side-track of Well B3. The Cook Formation was encountered oil-bearing (Wellbore: NPD FactPages).

2.1.2.2 Prospect B

The key study prospect B is penetrated by three wells. Well B1 is the key well for this study (Figure 4-8), located at the central part of the B prospect structure, discovered hydrocarbon(HC)-bearing Cook Formation in 2012 (Wellbore: NPD FactPages). The Well B1 is chosen as the key well based on the exhaustive data acquisition as well as extensive studies that have done. It was cored in the Upper part of the Cook Formation and comprehensively logged. The second target of the well B1 was Statfjord Formation, which was found water-bearing (Wellbore: NPD FactPages). The side-track of this well, B2 (Figures 4-8), which aimed to define the HC-water contact, proved hydrocarbon presence in the Cook Formation but contains minimum logging dataset (Wellbore: NPD FactPages). Finally, third well, penetrated the prospect at its southern part, is Well B3. This well confirmed the hydrocarbon presence as well as proved sands of better reservoir quality. Cores have been taken in the Lower Cook and the Well B3 in this study is used for 'Blind Test' (quality control of the final electrofacies model).

2.1.2.3 Prospect D

Prospect D is situated around 25 km North-North-East from B prospect (Figure 4). Three wells, D1, D2 and D3 are provided for the study. Well D1 discovered oil-bearing Cook Formation in 2008 at the northern part of the prospect (Wellbore: NPD FactPages). The core covers significant part of the Cook reservoir section. An oil appraisal well D2 has been drilled in order to delineate oil-water contact in the Cook reservoir, and confirm economic reserves presence (Wellbore: NPD FactPages). To the East from D structure, exploration Well D3 has been drilled to target the Cook and Statfjord reservoirs (Wellbore: NPD FactPages).

2.2 Methodology

2.2.1 INTRODUCTION TO THE METHODOLOGY

The methodology includes the following steps, which are described in details below and are shown at Figure 9;

1) Identification of available dataset and its preparation;
2) Quality control (QC) of the log data;
3) Preparation of the input set for the model
4) Generation of several unsupervised electrofacies models with Well B1 as the key (or reference) well;
5) Selection of most representative unsupervised electrofacies model after QC using conventional logs, litholog and PHIT generated from logs;
6) QC of the chosen key electrofacies model using core facies and depositional environment on Well B1;
7) Generation of supervised model and QC using available core facies;
8) Selection of the most adequate electrofacies model amongst unsupervised and supervised ones;
9) Propagation of the chosen model to other wells using Similarity Threshold Method (STM);
10) Correlation of propagated electrofacies on all wells;

If relation between electrofacies associations and sedimentary environment is proved:

- Paleogeographic reconstruction using electrofacies model
- Paleogeography model propagation over the other wells

11) Blind test on Well B3 of the propagated model.

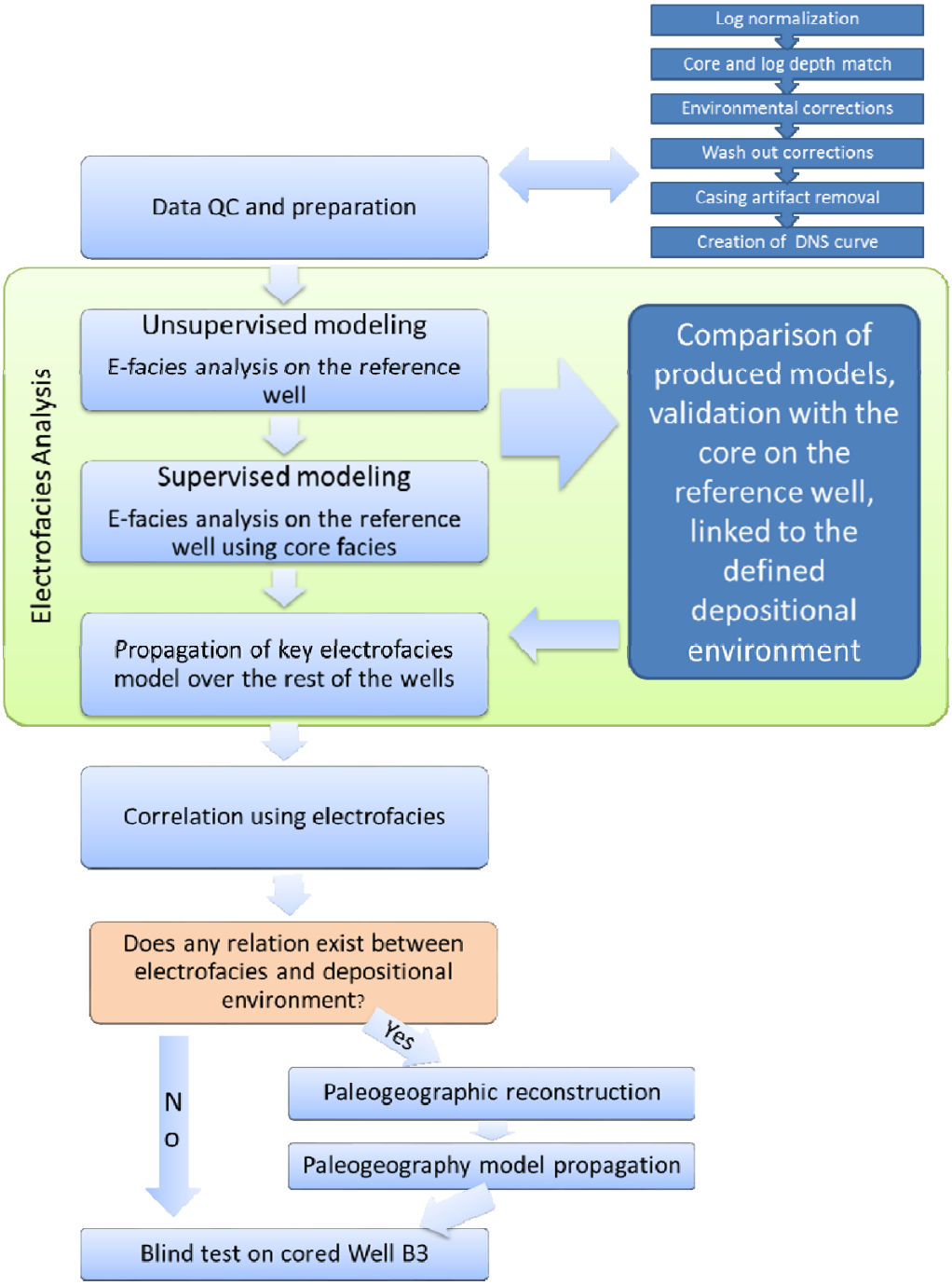

Figure 9: Simplified scheme of electrofacies analysis and related procedures

2.2.2 QUALITY CONTROL

It is very important to quality control the data and exclude any data that may not represent the petrophysics of the formation (Ramsin et al., 2009). These procedures usually include log normalization, environmental corrections where

necessary, wash out and despiking. In addition, abnormal well log responses may be revealed by statistical analysis. Figure 2 represents an example of final normalized log (GR) of the study wells.

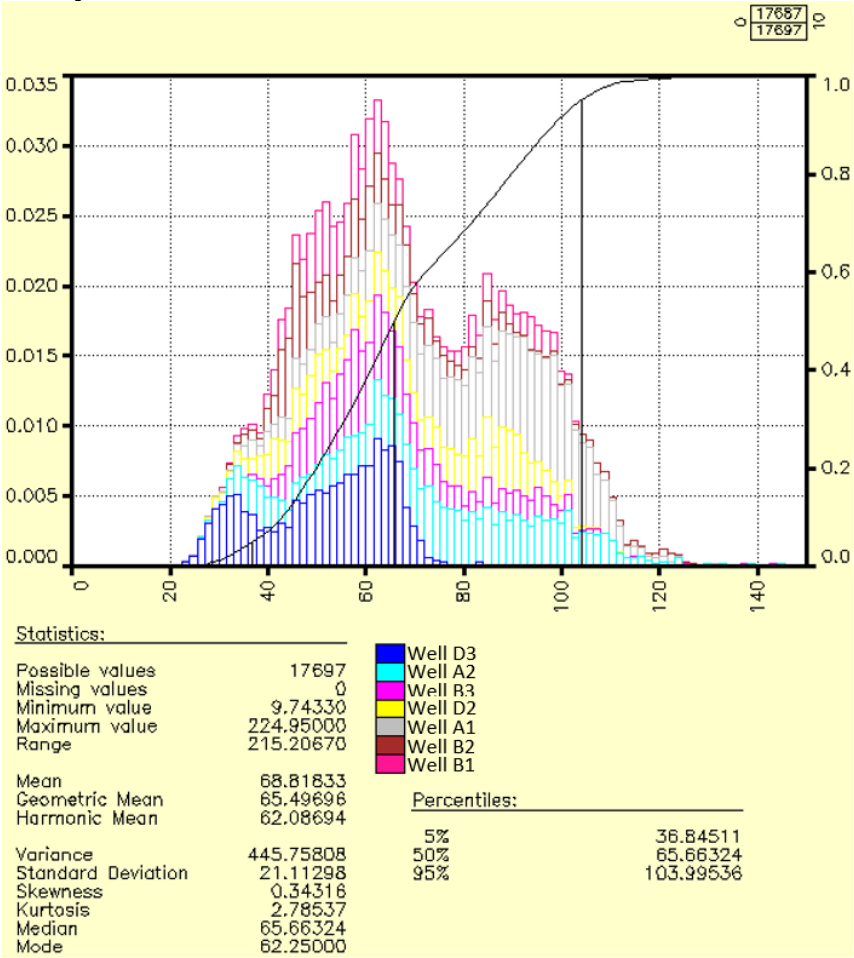

Figure 10: Normalized GR logs of the study wells (PDF and CDF) in API.

2.2.3 INPUT DATASET

Preparation of the input dataset, which contains all conventional wireline logs to be used. In addition to input dataset, core facies and image facies are defined by sedimentologist experts in Total E&P Norge (TEPN). The Cook reservoir layering is predefined and the depositional environment is been classified from core.

2.2.4 THEORETICAL FOUNDATION OF THE ELECTROFACIES ANALYSIS

Electrofacies analysis and most of the related steps are done with use of Multi-Resolution Graph-based Clustering (MRGC) technique available in Facimage application (advanced electrofacies analysis tool) of Geolog 6.7.1 (Formation Evaluation software).

Electrofacies modelling assumes definition of distinctive electrofacies (also simplified to "Facies" in the software; TEPN Internal Facimage manual) from clusters. Clustering is a specific term most commonly used as a mathematical technique for grouping of values in n-dimensional log space (Serra and Abbot, 1982). An n-dimensional space in electrofacies analysis comprises n-log dimensions, where each dimension is each log with its measurements distribution. The method of clustering implies classification of the data into local modes based on their natural characteristics of well log measurements that portray minerals and lithofacies within the logged interval (Lee et al., 2002; Rider and Kennedy, 2011).

In electrofacies analysis, the logging data from the cored well or wells constitute a "training set". On this logging set the relationships between logs and the core facies can be revealed (Doveton, 1994). Thus, model generated on the "training" set of the key Well B1, implies both as being the most trustful model, and containing core-log relationship information. Such model can be propagated to the rest of wells, and correlated across, allowing the prediction the rock properties, sedimentary facies, reservoir properties that would be seen in the cores, but must be derived from the logging curves (Doveton, 1994).

Final electrofacies are defined in two-step approach. At the first step, the log data are subdivided into a large number of clusters using MRGC. In a second step, one manually combines small clusters into electrofacies to which geological characteristics are assigned (Ye and Rabiller, 2000).

There are two methods of electrofacies modelling in terms of core facies usage that are applied in this study:

1) “Unsupervised” method;
2) “Supervised” method

Unsupervised electrofacies modelling allows data exploration without limiting it with predefined classes. Thus, the method is designed to reveal natural structure of the data (Doveton, 1994) and group it according to predefined requirements, e.g. clusters with specific range of porosity, and clusters of cemented sandstones.

Supervised electrofacies modelling use of groups specified before the analysis (Doveton, 1994). Structural information is defined to optimize the match between original data (for instance, core facies) and produced electrofacies.

The available INPUT_GEOL data herein referred to as “training data” and can be viewed as frequency distribution in the form of histograms. Statistical information display of the minimum (MIN), maximum (MAX), standard deviation (STD DEV), mean (MEAN) of the input data as well as the end limits can easily be seen on the histogram plots on Figure 11. On this figure, ‘Model Logs’ in the software are main logs, used in the study, and ‘Associated Logs’ are those, which provide additional information. Main logs together with associated logs are the source data for electrofacies models.

There are several possible techniques of clustering and available, namely,

- "Dynamic Clustering"
- "Ascendant Hierarchical Clustering (AHC)"
- "Self-Organizing Map Clustering (SOM)"
- "Multi-Resolution Graph-Based Clustering (MRGC)"

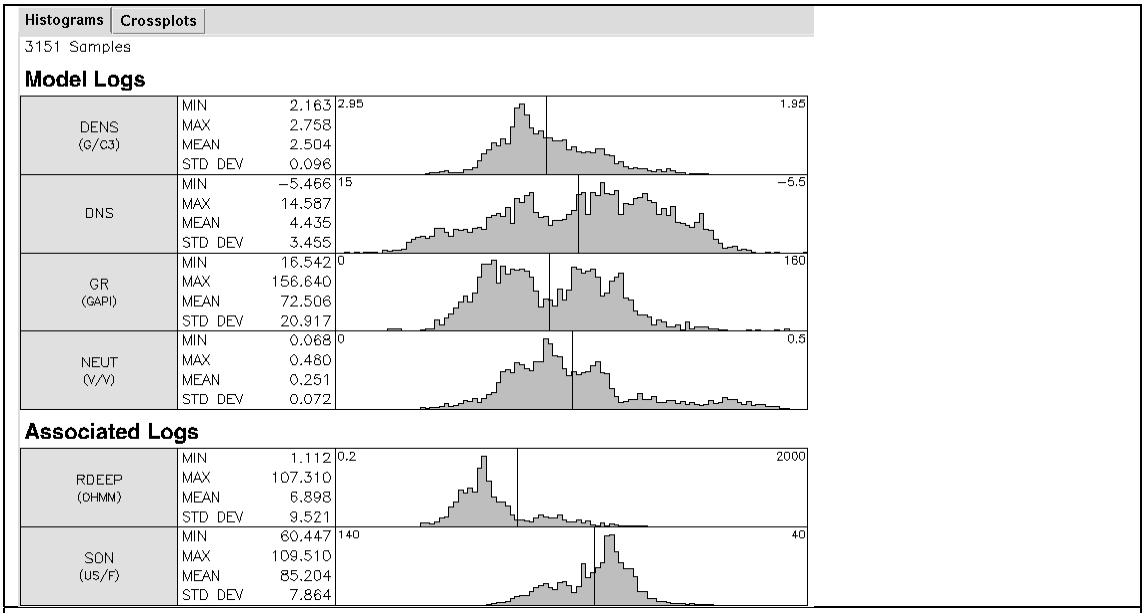

Figure 11: Input logs, and values distribution (grey histograms). Min – minimum, Max – maximum, Std Dev – standard deviation values of each log dimension.

Dynamic clustering and AHC provide grouping of log values by their proximity not including information of natural density patterns, unlike method invented by Ye and Rabiller (2000) particularly for the electrofacies analysis. In this study, the MRGC technique is used for unsupervised electrofacies modelling.

MRGC – Multi-Resolution Graph-Based Clustering method analyses the underlying structure of the data. First, clusters are identified by a "neighbouring index" of each log measurement point in the data set (Ye et al., 2001). This index indicates how strong a point attracts or get attracted by other points (Ye and Rabiller, 2000). Then, small group of points are designed using K-Nearest-Neighbour approach. In order to define optimal amount of clusters within user-specified resolution Kernel Representative Index (KRI) is utilized. Thus, MRGC produces optimal amount of cluster models according to defined requirements. Benefits and details of the MRGC methodology are thoroughly described in patent article of Ye et al. (2001) and article published by Ye and Rabiller (2000).

Automatically generated MRGC models differ by amount of clusters they contain, what is reflected in the name of each model. In order to choose the optimal model, Facimage allows viewing properties of each model, including component clusters, log values assigned to each cluster, and comparison of a selected model with any other model or with associated log by statistical approach.

Clusters can be graphically viewed and manipulated using cross-plots and histograms, which is the most convenient approach during this study workflow. Optimal facies arrangement is a result of an iterative process of MRGC modelling, clustering process (grouping and splitting clusters), and propagation to the key well, until electrofacies will reflect all the necessary heterogeneity, changes in depositional environment, and will be able to pick the most significant cemented zones.

At the stage of model propagation, Similarity Threshold Method (STM) is used. It is a tool that allows comparing the reference dataset (model logs dataset from the key well) to application dataset (model logs dataset of the rest of the wells) at the final electrofacies model propagation stage over the rest of the wells (TEPN Internal Facimage manual). Particularly, STM technique displays intervals, where application log data stands out of the corresponding log range from the reference dataset. Hence, the propagated electrofacies quality may be evaluated.

3 EVALUATION

3.1 Key Well Modelling

Electrofacies modelling on the key Well B1 is done by unsupervised and supervised methods consecutively.

3.1.1 UNSUPERVISED MODELLING

3.1.1.1 Preparation to the clustering

The key well model is crucial for the later steps of electrofacies analysis, as it forms a basis for most of the results in this study. The electrofacies analysis starts with Facimage project definition, specification of the Model and Associated Logs, and setting of end limits of the logs. The data specified in input logs are used to create training data for the electrofacies models (TEPN Internal Facimage manual). Figure 12 shows the input logs set with an example of log (RHOB) end limits.

Associated Logs chosen for unsupervised modelling are Sonic and Resistivity Log (Figure 13); however, these logs are included rather as an additional input dataset to aid on lithological calibration for the purpose of facies prediction. It is worth noting that Resistivity Log is affected by fluids, and therefore, including this log into modelling could distort clustering. In addition, there is limited acoustic impedance between Cook sandstones and Intra-Cook shales, therefore Sonic Log usage is restricted. Both logs are used together with NP and RHOB logs for prediction of the cemented zones.

A combination utilizing the training data is used for generation of cross-plots (Figure 14) and histograms (Figure 15) that represent a graphical summary of the logs and relationships between them. The main cross-plots for electrofacies analysis utilized in this study are RHOB versus NP (RHOB-NP cross-plot) and DNS versus GR (DNS-GR cross-plot) logs as shown on Figure 16. The combination using all the

aforementioned cross-plots approach gives good control and better understanding of the predicted groups of facies.

Figure 12: Model logs: RHOB settings.

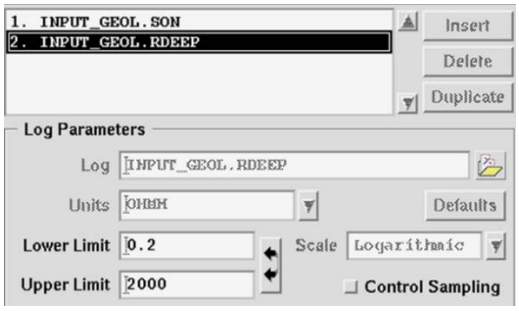

Figure 13 Associated Logs: Resistivity Log settings

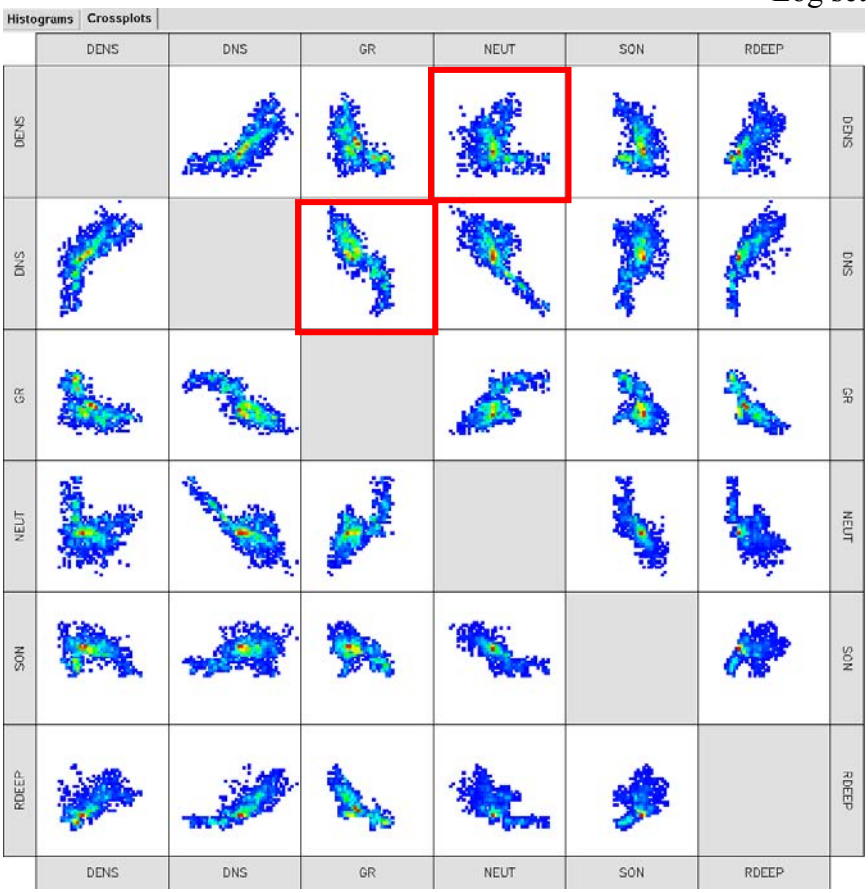

Figure 14: Cross-plot summary displays for specified Model and Associated Logs. The colour in the cross-plot views displays the frequency values using the default Rainbow colourmap (TEPN Internal Facimage manual). Red squares show two the most common cross-plots (RHOB-NP and DNS-GR).

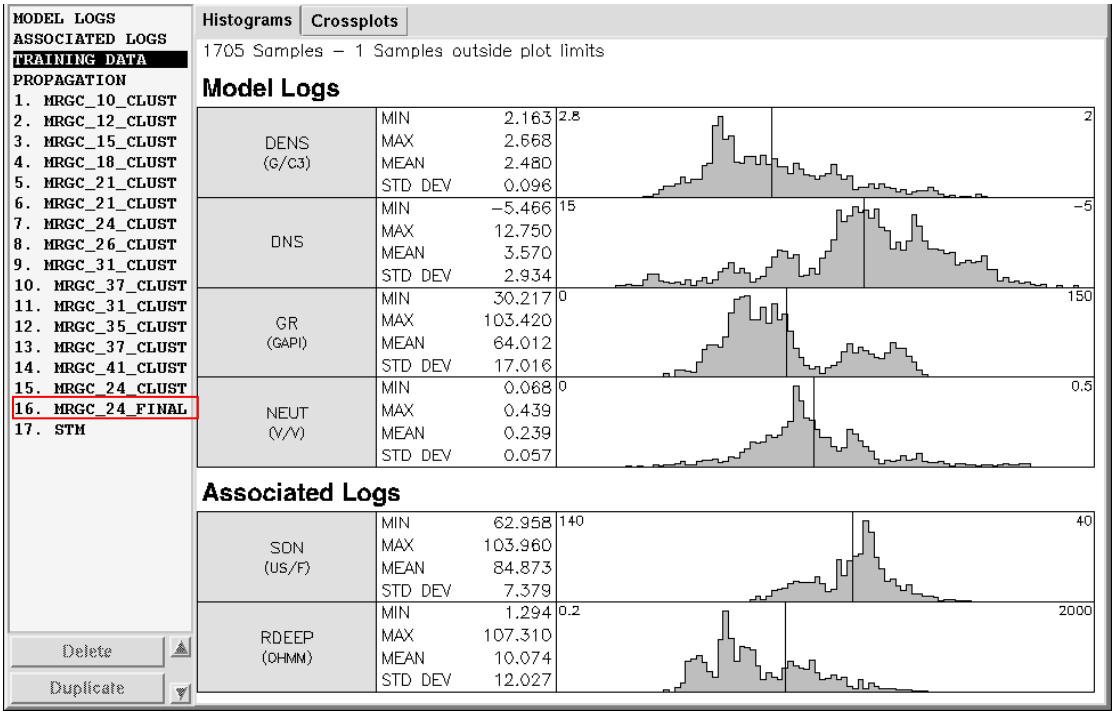

Figure 15: Modelling data represented on histograms. MRGC model in red rectangular is the final electrofacies model.

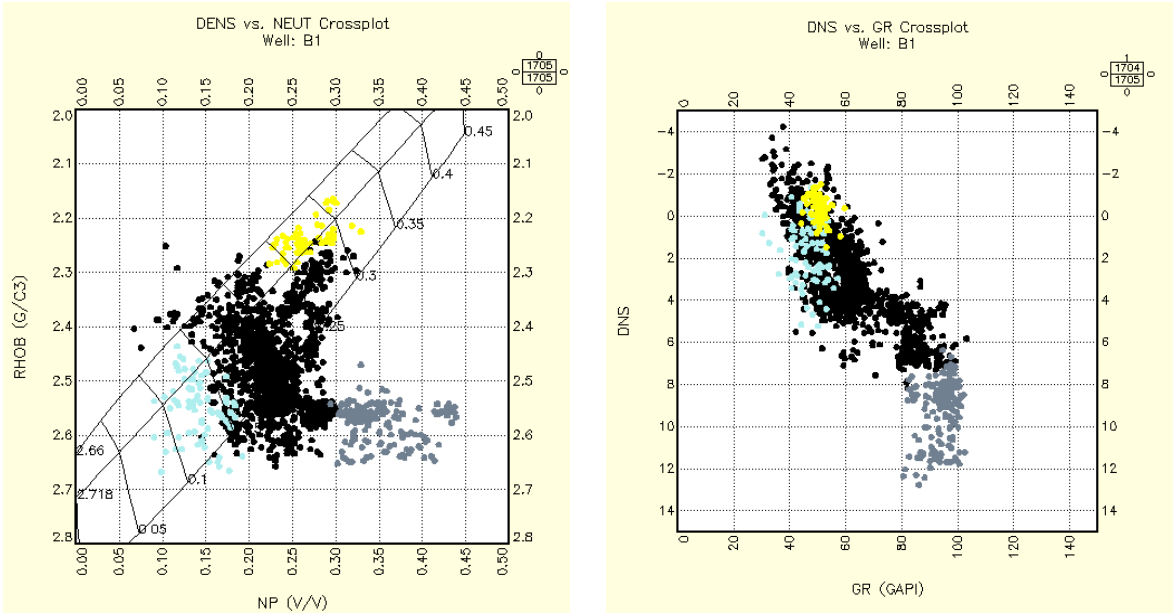

Figure 16: Left cross-plot is RHOB versus NP; right plot is DNS versus GR. Yellow dots are high porosity, low GR sandstones; blue dots are low porosity cemented sandstones and silts; grey dots are low porosity shales with high GR reading.

3.1.1.2 Cluster Analysis

A total of 24 initial clusters are created from the key well B1, which are then regrouped to create a composite unsupervised electrofacies model containing 12 electrofacies. Electrofacies table represented on Figure 17 shows final groups of electrofacies, with their assigned names and colours according to their properties.

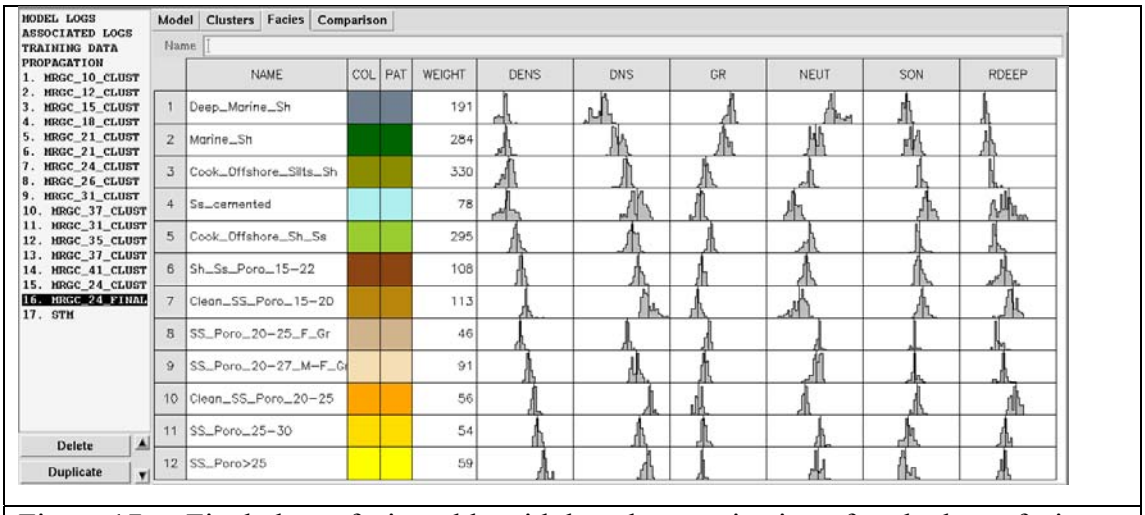

Figure 17: Final electrofacies table with log characterization of each electrofacies.

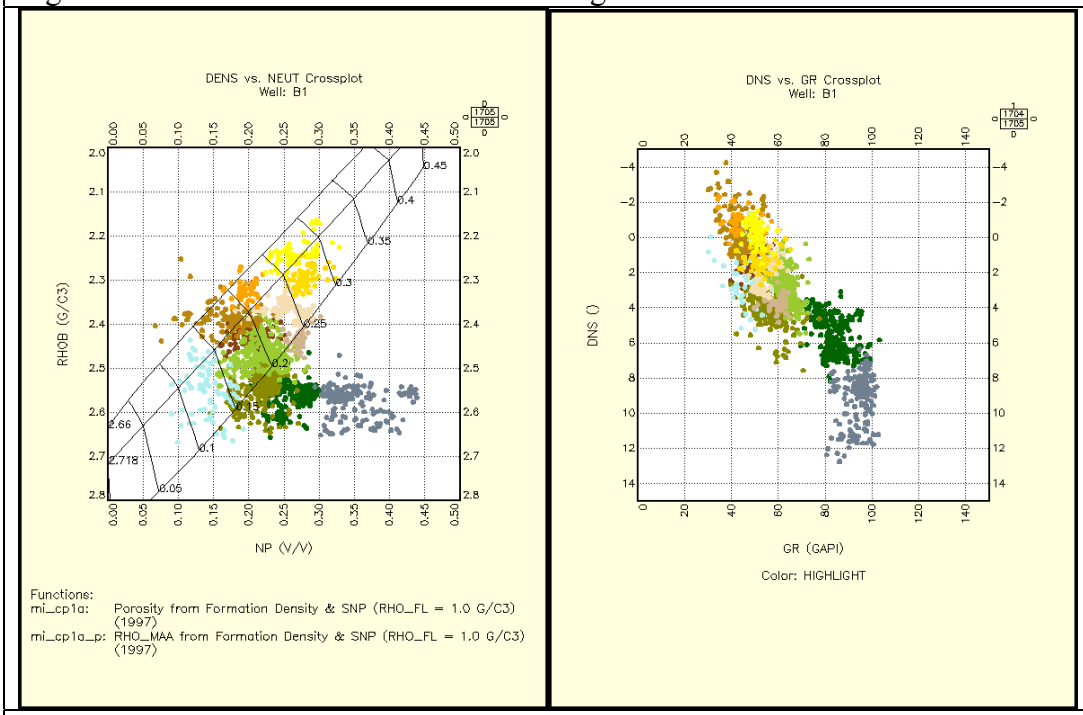

Figure 18: Final electrofacies distributed in RHOB-NP (left) and DNS-GR (right) cross-plots.

Electrofacies #1-3 (EF#1, EF#2, EF#3) and electrofacies #5 (EF#5) are mainly shales, electrofacies #4 (EF#4) represents cemented intervals, and electrofacies #6-12 (EF#6, EF#7, EF#8, EF#9, EF#10, EF#11, and EF#12) show different variations of sandstones (Figure 17).

Shaly EF#1-3 have relatively high GR reading, high NP values together with high RHOB. It is assumed, the higher the GR and NP reading, the more shaly sediments are.

Cemented intervals are marked by EF#4. In order to better characterize and define its limits, the sonic and resistivity logs were introduced. A relatively low GR reading (API), low NP, high RHOB (g/cm^3), high DT (US/F) together with high Resistivity Log (with high water saturation (Swo)) are featured cemented intervals. An approach integrating all five logs (GR, NP, RHOB, DT, RT) together with the lithologs, is used as additional calibration of cemented intervals. The most significant cemented stringers are grouped in electrofacies.

Electrofacies #5 represents Intra-Cook shales, with similar characteristics to silts, but a higher clay content.

EF#6-9 correspond to silty-sand facies with varying clay-content, grain size and DNS, while the GR reading is of less importance. The high GR measurements can be explained by variable mica and K-Th content in sandstones.

EF#10-12 show the best porosity zones and low clay content with a low DNS as compared to EF#6-9. The most significant observation in the sandstone facies clustering, is distinct porosity that can help to disclose heterogeneity in reservoir sandstones.

3.1.1.3 Shales and Reservoir layering versus Electrofacies.

Figure 19 and Table 3 summarizes correspondence of the modelled electrofacies with input log data, layers, litholog and log computed PHIT. Appendix 1-6 displays facies tables with corresponding model and associated logs statistic.

Amundsen Formation is known as shallow marine shelf deposited (Lithostratigraphy: Amundsen Formation, NPD FactPages), and is characterised by mainly shaly EF#3, interplay of EF#5, #6 in the lower part of the formation, unlike the upper part is dominated by EF#2 and EF#5. Cemented intervals are recognized by EF#4.

Burton open marine shales (Lithostratigraphy: Burton Formation, NPD FactPages) are defined dominant presence of EF#2 and EF#3.

An internal layering of the Cook formation subdivides it into seven reservoir layers based on sedimentological and stratigraphic interpretations by TEPN experts.

Cook 1 corresponds to the basal forced regressive wedge of the Cook Sandstone. It consists mostly of tidal, mouth bars and foreshore facies, with a few channels (TEPN – Well B1 Confidential Report, 2014). On logs they appear to be silts, silty sands which is as defined by EF #3, #6, #7 with presence of well defined cemented intervals that are clearly distinguishable by EF #4. Cook 1 is capped by a widespread flooding surface seen at the base of Cook 2.

Cook 2 corresponds to the base of the lowstand wedge of the Cook, above the Cook Maximum Regressive Surface (CMRS) (TEPN – Well B1 Confidential Report, 2014). It should be made up of amalgamated deltaic distributary channels and sand flat deposits (TEPN – Well B1 Confidential Report, 2014), and is predominantly characterized by EF#7. The channels with good porosity (17-22%) are defined by EF#10 while the Intra-Cook cemented interval is captured by EF#4. It is capped quite sharply by a thin (3m) shalier unit which marks the onset of late lowstand aggradation.

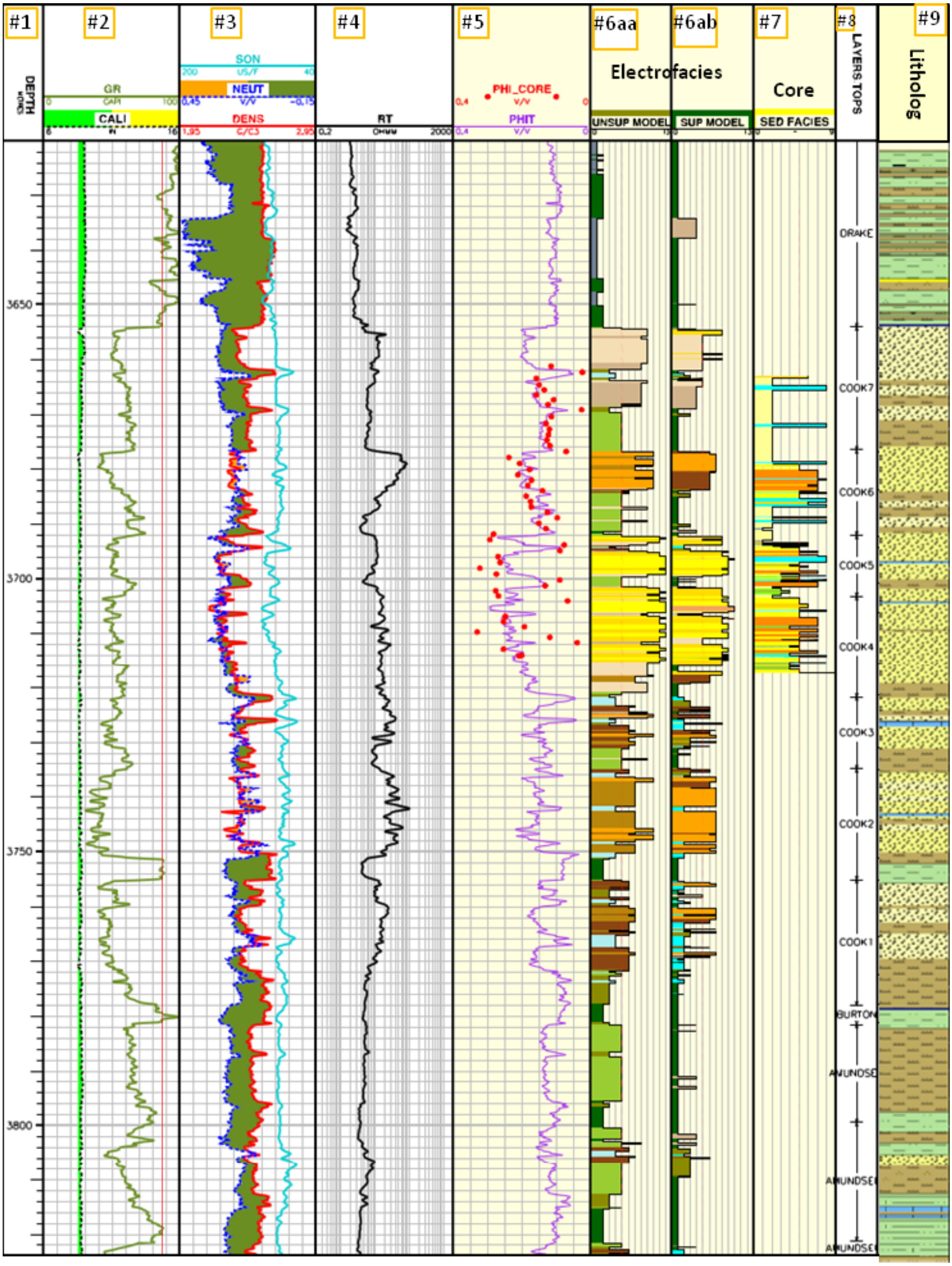

Figure 19: Key Well B1 with input and associated logs, electro-, core facies, formation tops, layering, and litholog. The first track to the ninth track is TD (m), GR (1-100 API)-Caliper (0-16 In), SON (200-40 US/F)-PEF (0-20 B/E)-NP (0,45-(-0,15) V/V)-RHOB (1,95-2,95 G/C^3), RT (0.2-2000 OHM*M), Core porosity (PHI_Core, 0.4-0)-PHIT (0.4-0), Key Well B1-based unsupervised electrofacies log, Key Well B1-based supervised electrofacies log, Core facies, formation layering, Litholog.

Table 3: Electrofacies of unsupervised modelling and their main log and PHIT distinctive characteristics with no extreme data points taken into account

#	Facies name	Poro	GR (API)	DNS	NP	RHOB (g/cm^3)
1	Deep_Marine_Shales_GR>80	n/a	80-100	>6	0.30-0.44	2.53-2.65
2	Marine_Shales_05<Por<08	n/a	60-100	+4 - +6	0.22-0.30	2.52-2.61
3	Silts&Shales_48<GR<64	0.17-0.22	48-64	+2 - +6	0.17-0.25	2.46-2.63
4	Cemented	0.07-0.15	30-50	-1 - +4	0.10-0.16	2.45-2.67
5	Intra_Cook_Shales_avg_Por10	0.15-0.23	50-70	0 - +4	0.16-0.25	2.37-2.52
6	Shaly_Sandstones_avg_Por15	0.17-0.22	40-60	0 - +4	0.16-0.25	2.40-2.47
7	Silty_Sandstones_15<Por<20	0.15-0.20	30-50	-4 - +2	0.12-0.22	2.35-2.44
8	Shaly Sandstones_51<GR<65_&_Por14	0.23-0.25	51-65	+3 - +5	0.25-0.28	2.40-2.47
9	Shaly Sandstones_48<GR<56_&_Por18	0.20-0.27	48-56	0 - +4	0.22-0.29	2.32-2.40
10	Sandstones_avg_Por19	0.20-0.23		-2 – 0	0.16-0.22	2.29-2.36
11	Shaly_Sandstones_25<Por<30	0.25-0.30	40-60	0 - +3	0.25-0.30	2.24-2.34
12	Clean_Sandstones_Por>25	>0.25	40-60	-2 - +1	0.22-0.30	2.16-2.29

Cook 3 is characterized by strong calcite cementation with heterogeneous intervals that is defined by EF #6, EF#7, and EF#9. The Intra-Cook shale is distinct in this layer and is characterized by EF#5 with the cemented zones as EF#4. According to TEPN – Well B1 Confidential Report (2014) the top of Cook 3 is defined by a subtle Intra-Cook flooding surface (ICFS3).

Cook 4 should be made up of a complex amalgamation of shallow channel fills and tidal bar sand bodies with varying ranges in porosity (TEPN – Well B1 Confidential Report, 2014). The lower part consist of shaly sands dominated by EF#7, EF#9 while the upper part consist of better reservoir quality sands with porosity ranging between 25-30% and corresponds mainly to facies EF#11 and EF# 12.

Cook 5 is quite thin; it represents the first backstepping wedge of the Transgressive Systems Tract (TST). It is capped by a sharp marine ravinement surface (TEPN – Well B1 Confidential Report, 2014). From core data, it is made up of stacked tidal bars, with limited potential of erosional amalgamation (TEPN – Well B1 Confidential Report, 2014). It is dominated by high porosity facies EF#11 and EF# 12 while the Intra-Cook shales where present are represented by EF#6 and EF#7.

Cook 6 is the second backstepping wedge of the TST. It capped by a sharp erosional wave ravinement surface as well. In terms of reservoir, the cleanest sandstone found at the top corresponds to upper shoreface or foreshore deposits (TEPN – Well B1 Confidential Report, 2014) and is defined by EF#10. In contrast to the tidal facies, which show small scale variation in reservoir quality and several scales of shaly heterogeneities, the foreshore appears to be more homogeneous, with progressive lateral degradation as characterized by EF#7. The basal part of Cook 6 consists of a more shaly interval dominated by EF#5 and the progradational trend is seen on logs as a funnel pattern.

Cook 7 is the third and last backstepping wedge of the TST. It is capped by a major regional flooding surface (TCFS) that marks the top of the Cook below the Lower Toarcian Drake shale (TEPN – Well B1 Confidential Report, 2014). Layer 7 has almost no good quality reservoir sands, with too distal neritic or shoreface facies. This shoreface layer is sub-characterized by three different possible environments, namely; middle shoreface, lower shoreface and Intra-Cook shale. These three subdivisions are also depicted during the electrofacies study to correspond predominantly to EF#, 9 EF#8 and EF#5 respectively.

Drake shales are known to have been accumulated in deep marine anoxic environment (Lithostratigraphy: Drake Formation, NPD FactPages). It is dominated by EF#1, which is clearly not identified in any other formation.

3.1.1.4 Calibration to core facies

Core covers layers Cook 4 - Cook 7, while sedimentary facies are additionally defined from image logs for a wider range in the Cook Formation (TEPN – Well B1 Confidential Report, 2014). Therefore, calibration electrofacies (EF) to core facies is performed on main reservoir Cook sandstones and does not include deep marine offshore EF#1 in the Drake interval. Table 4 summarizes the analysis, where each core facies correspond to a family of electrofacies with assigned approximate probability.

Core Facies 1 (CF1): Bioturbated silty shale.

This facies is made up of grey beige silty shale showing intense bioturbation on cores. These deposits are interpreted as shallow marine lower shoreface or upper offshore deposits, where the initial alternation of muddier fair-weather deposits and silty to sandy storm beds were completely mixed by pervasive burrowing (TEPN – Well B1 Confidential Report, 2014). They correlate to EF#2 and EF#5.

Core Facies 2 (CF2): Bioturbated sandstone.

This facies corresponds to massive well-sorted fine-grained beige sands showing a densely burrowed texture. This facies corresponds to a shoreface depositional environment in transgressive or regressive settings. Intense burrowing and cross-stratification (hummocky and swaley type) indicate these settings respectively (TEPN – Well B1 Confidential Report, 2014). These sandstones calibrate with EF#5 and EF#8.

Core Facies 3 (CF3): Heterolithics.

This facies is not much represented. It shows a centimetric to decimetric alternation of fine to medium grained sandstone beds and thin shaly interbeds. The bedding is horizontal to wavy, disrupted by significant and diverse burrowing. This facies is interpreted as tide dominated bay to “deep estuarine” deposits.

Table 4: Core facies correspondence to electrofacies. Core facies and description is from internal sedimentary studies report (TEPN – Well B1 Confidential Report, 2014)

Core Facies	Description	Probability	Electrofacies #	Electrofacie Description
CF1	Bioturbated silty shales (shales to siltstones) made up of grey beige silty shale showing intense bioturbation, and is interpreted as shallow marine lower shoreface, upper offshore deposits.	Most likely	**2**	Marine_Shales_05<Por<08
			5	Intra_Cook_Shales_avg_Por10
CF2	Bioturbated sandstones are massive well-sorted fine-grained beige sands, accumulated in shoreface settings.	Most likely	**5**	Intra_Cook_Shales_avg_Por10
			8	Shaly Sandstones_51<GR<65_&_Por14
		Minor appearance	3,9	
CF3	Shaly and sandy heterolithics, deposited in tide-dominated bay to "deep estuarine" environment.	Most likely	**5**	Intra_Cook_Shales_avg_Por10
		Minor appearance	**12**	Clean_Sandstones_Por>25
CF4	Horizontal to wavy-bedding sandstones with mud drapes and flakes, are interpreted as subtidal deposits in protected environment with no wave action.	All the e-facies appear equally	**8**	Shaly Sandstones_51<GR<65_&_Por14
			9	Shaly Sandstones_48<GR<56_&_Por18
			11	Shaly_Sandstones_25<Por<30
			12	Clean_Sandstones_Por>25
CF5	Cross-bedded well-sorted medium to fine sandstones with mud drapes, deposited in shallow subtidal to intertidal environment.	Most likely in Upper Cook	**10**	Sandstones_avg_Por19
		Most likely in Lower Cook	**11**	Shaly_Sandstones_25<Por<30
			12	Clean_Sandstones_Por>25
		Minor appearance	6,7,8,9	
CF6	Clean horizontal to wavy-bedding with mud drapes and flakes are deposits of a shallow coastal setting with permanent wave action, possibly in a tidal sand flat ro foreshore settings.	Mixed	2, 5, 9, 10, 11, 12	
CF7	Clean sandstones with cross-bedding are deposited in foreshore of shallow tidal channel deposits.	Most likely in Upper Cook	**10**	Sandstones_avg_Por19
			7	Silty_Sandstones_15<Por<20
		Most likely in Lower Cook	**9**	Shaly Sandstones_48<GR<56_&_Por18
			11	Shaly_Sandstones_25<Por<30
			12	Clean_Sandstones_Por>25
CF8	Calcite cemented sandstones are distinctive calcite cemented intervals. Calcite cement may be linked to the secondary reprecipitation.	All the e-facies appear equally	**4**	Cemented
			5	Intra_Cook_Shales_avg_Por10
			6	Shaly_Sandstones_avg_Por15
		Mixed	7,8,9,10,11,12	

It may corresponds to the bottomsets of tidal bars (TEPN – Well B1 Confidential Report, 2014). Generally, these heterolithics match with Intra-Cook shales, EF#5.

Core Facies 4 (CF4): Wavy-bedded sandstone with mud drapes

This facies is transitional with CF3 with a loss of the shaly fraction and a moderate burrowing. The grain size is fine to medium, with a moderate sorting and few coarser lags. Shale is present as discontinuous drapes or thin laminae instead of interbeds. The irregular wavy bedding is only slightly deformed. Small calcitised patches are observed at places. It is interpreted as subtidal deposits in a protected environment without wave action (TEPN – Well B1 Confidential Report, 2014). CF 4, wavy-bedded sandstones with mud drapes coincides with a complex of four 'sandy' electrofacies #8, #9, #11, #12.

Core Facies 5 (CF5): Cross-bedded sandstone with mud drapes

This facies is made up of moderate to well-sorted medium to fine sandstone with steeply dipping (>15°) laminae underlined by thin mud drapes. The individual sets of cross-beds are 10 to few 10s of cm thick. Mud-draped cross-beds are nearly diagnostic of a shallow subtidal to intertidal environment. This facies records the migration of shallow tidal megaripples and bars in a "protected" tidal sand flat to estuarine setting (TEPN – Well B1 Confidential Report, 2014). CF5 have different correlation with electrofacies in the Lower and Upper Cook. In the Lower Cook they correspond to #11, #12 with minor appearance of other 'sandy' electrofacies, and in the Upper Cook – to the 10^{th} electrofacies.

Core Facies 6 (CF6): Horizontal to wavy-bedded clean sandstone

This facies is comparable to CF4 but with very little clay. Only a few laminae or flasers are found. Detailed observation of sedimentary structures is hampered by the strong dark oil staining. In a shallow coastal setting, the near absence of slack-water clay drapes suggests a permanent wave action, possibly in a tidal sand flat to foreshore setting (TEPN – Well B1 Confidential Report, 2014). There is no clear

trend of electrofacies and CF 6 correlation, probably due to the CF6 occurrence in diverse depositional environment.

Core Facies 7 (CF7): Clean cross-bedded sandstone

This facies is comparable to CF 5, with large sets of oblique laminae, but with almost no clay drapes. Observed trough cross-bedding is believed to be produced by the migration of sinuous megaripples. To the lack of clay drapes indicates permanent energy, most likely due to wave action. This facies should correspond to foreshore or shallow tidal channel deposits (TEPN – Well B1 Confidential Report, 2014). CF 7 as well as CF 5 have two various electrofacies complexes for the Lower Cook (#9, #11, #12) and Upper Cook (#7, #10), however most of the mentioned electrofacies represent high porosity sandstones.

Core Facies 8 (CF8): Calcite-cemented sandstone

CF 8 represents calcite cemented intervals rather than sedimentary facies. The calcite cement may be linked to reprecipitation around intervals with initial high concentrations in shell debris. Thorough calcite cementation is observed as overprints on all types of facies. CF8 was assigned to the intervals that has thickness over 5 cm (TEPN – Well B1 Confidential Report, 2014). CF8 coincides both with electrofacies #4 and shaly facies #5 and #6. In addition, all other sandy electrofacies may concur to the CF 8.

3.1.1.5 Calibration to depositional environment

Sedimentary facies are assigned to each depositional environment as defined within the Cook Formation with an assumption of some uncertainty degree in interpretation. As seen from the Figure 20 there is some degree of depositional environment, electrofacies associations and core facies relationships. These relationships are used when paleogeographic reconstructions are conducted.

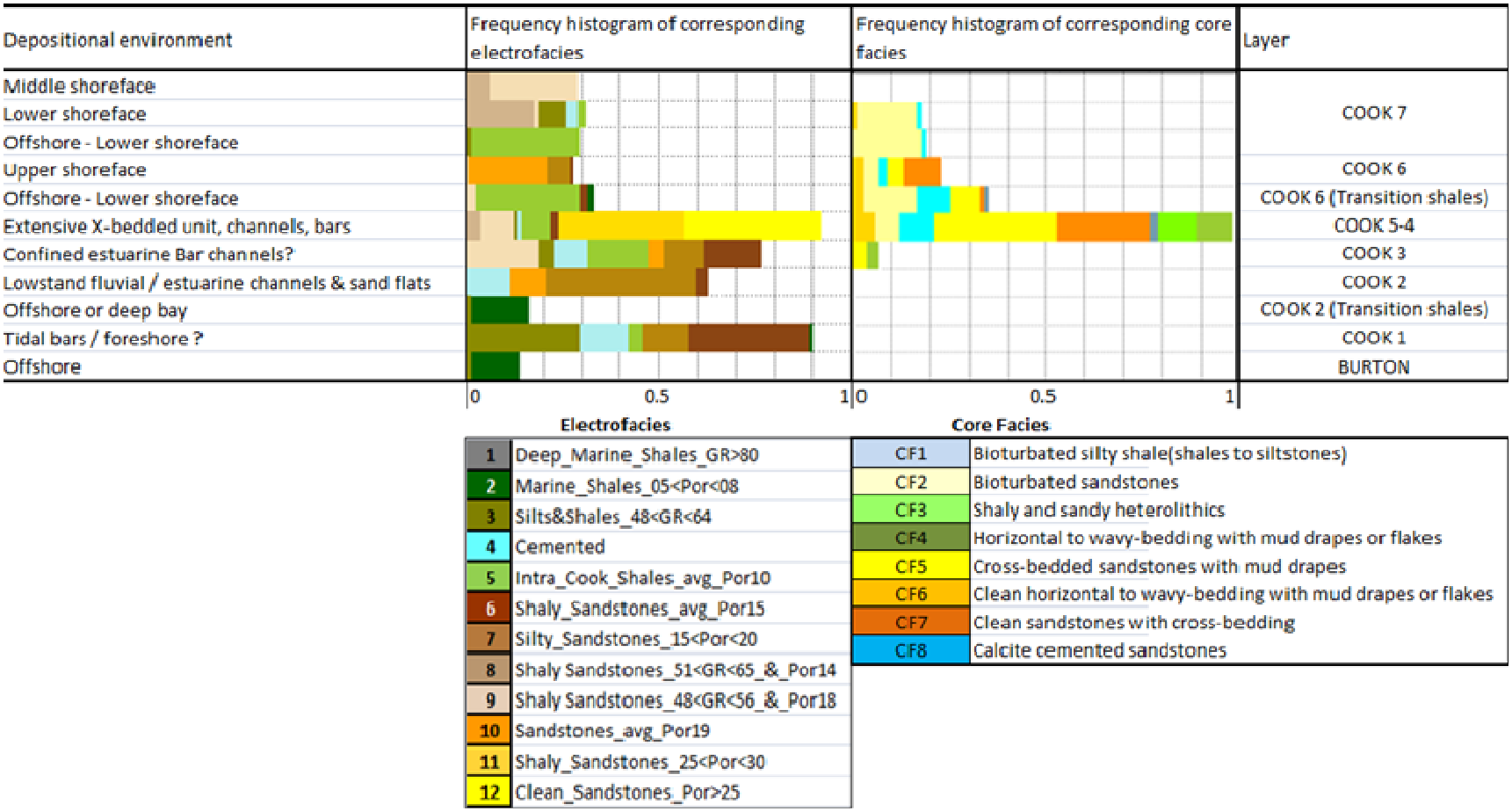

Figure 20: Depositional Environment, Electrofacies and Core Facies correspondence

3.1.2. SUPERVISED MODELLING

Eight core facies defined in the key well B1 form a base for electrofacies definition during supervised modelling. Thickness analysis of using the 8 core facies with a tool resolution 0.2" as a constrain is represented on Table 5.

3.1.2.1 Thickness cut-off

Some core facies (e.g. #2, #5, #7 and #8) have been described in beds largely thicker than log vertical resolution, and therefore have a chance to be identified using conventional logs. Other facies (e.g. #1, #3 and #4) systematically occur in beds thinner that log vertical resolution. As a result, thin facies are mostly not included into electrofacies modelling.

3.1.2.2 Preparation to the clustering

Training data includes the same model logs as in unsupervised modelling (RHOB, NP, GR, DNS), while associated logs used for the modelling are core facies evaluated in thickness cut-off analysis and a log that filters these facies (Figure 21 and Figure 22). From model logs data range and points quantity it is obvious that information exceeding core coverage is not included into modelling, for example, deep marine shales of the Drake Formation, which has GR over 75 API. Furthermore, Facies associated log shows that core facies #1 (Bioturbated silty shales), #4 (wavy-bedded sandstones with mud drapes) are not included into modelling, and core facies #3 (heterolithics) and #6 (horizontal to wavy-bedded clean sandstones) are represented by little data (Figure 22).

Table 5: Core facies thickness analysis. Histograms #1-8 correspond to 8 core facies thickness distribution respectively. Red dashed line represent thickness cut-off=0,2m

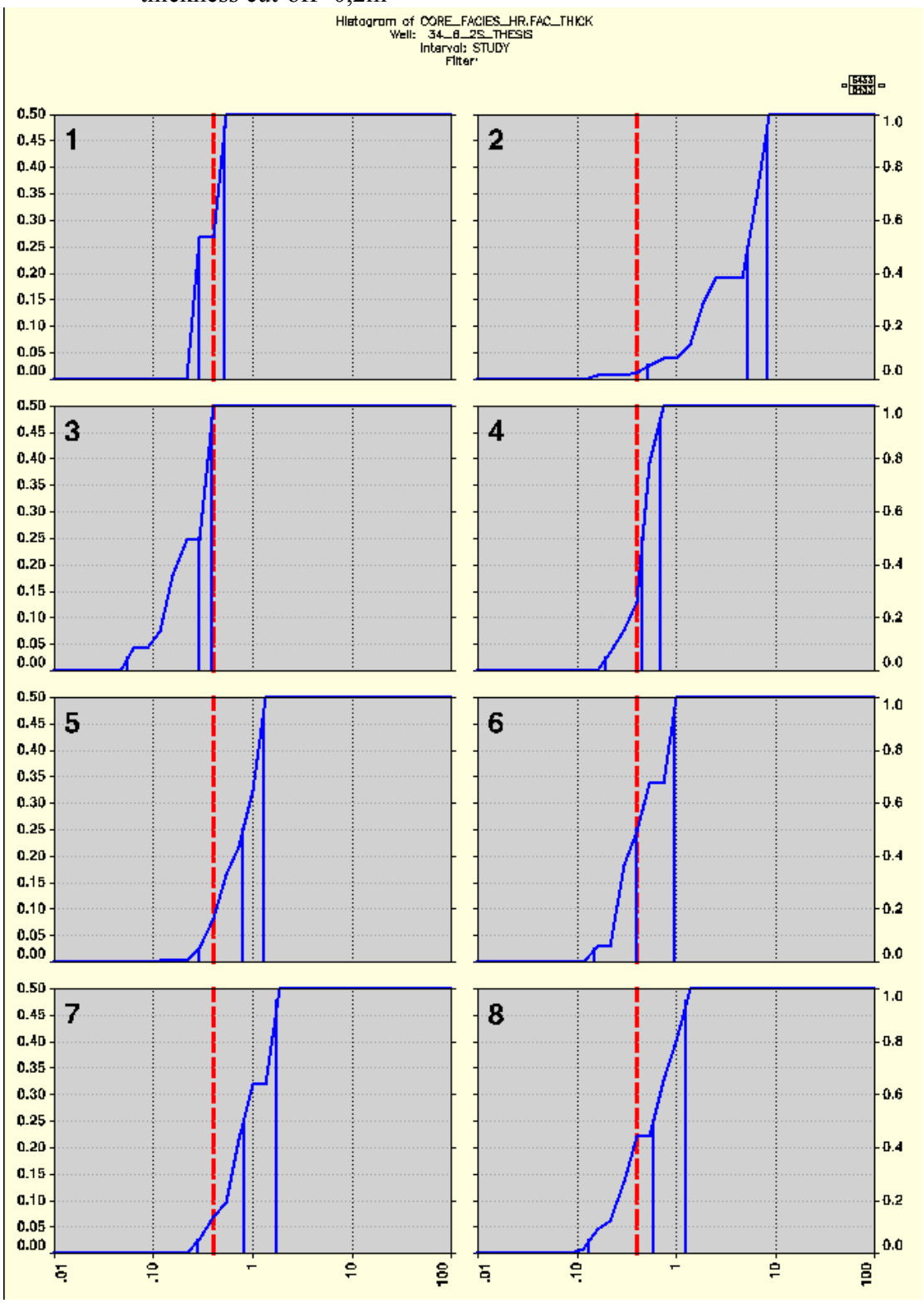

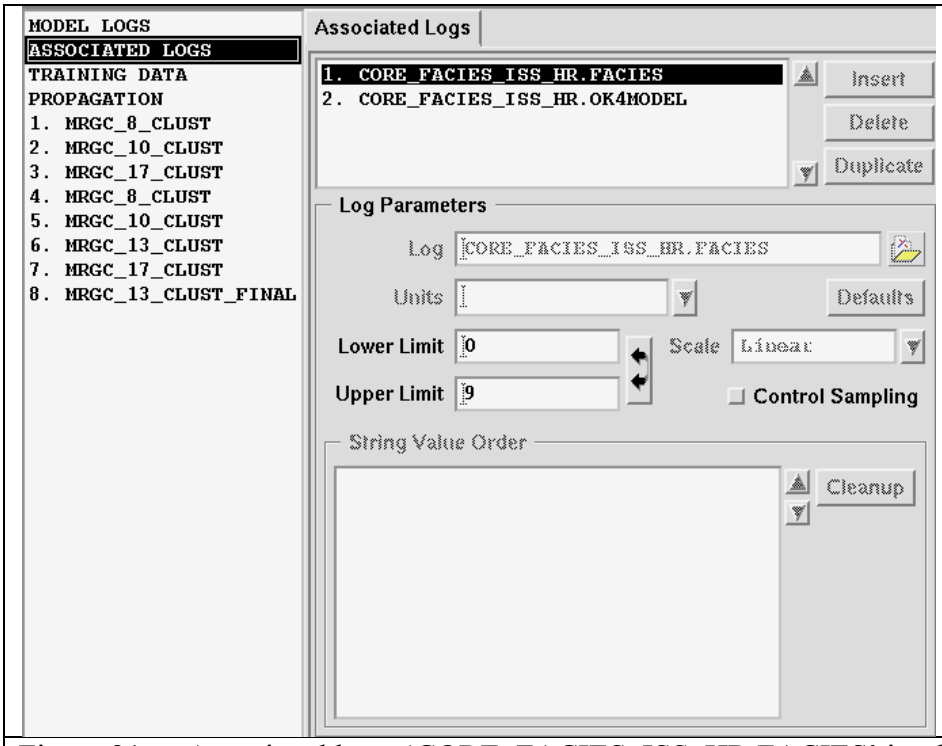

Figure 21: Associated logs. 'CORE_FACIES_ISS_HR.FACIES' is s log of 8 core facies, 'CORE_FACIES_ISS_HR.OK4MODEL' is a facies thickness cut-off filter.

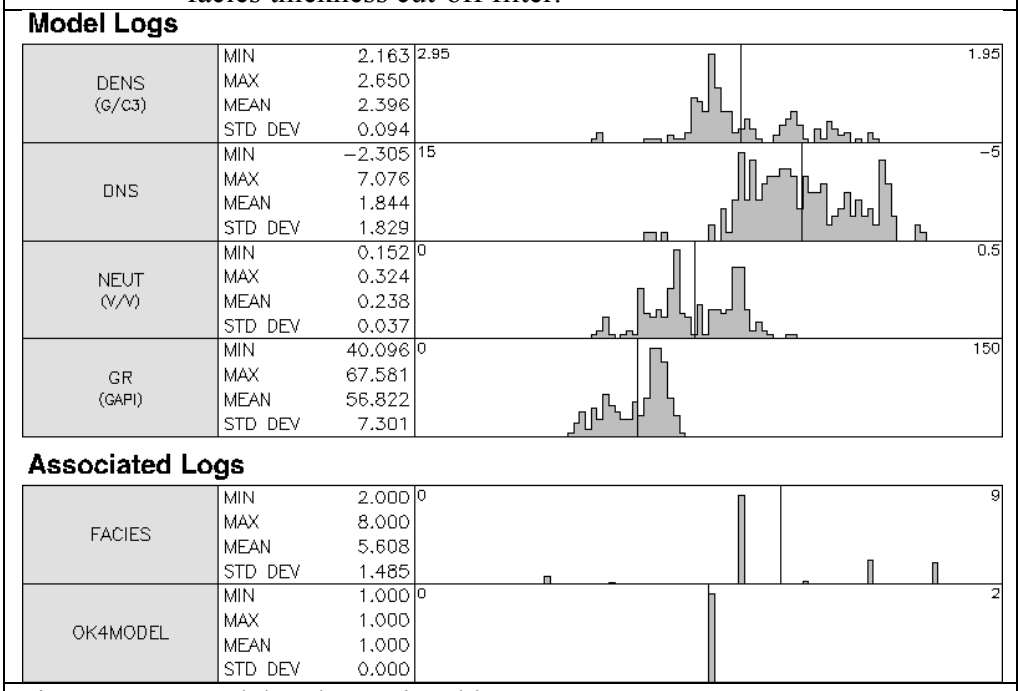

Figure 22: Model and associated logs.

3.1.2.3 Cluster analysis

Final supervised model is represented on facies table (Figure 23), and as a log on track #10 on Figure 19. The model is built from 13 cluster MRGC model, and contains 10 final electrofacies. EF #1 and #3 are linked to shales and shaly sandstones, EF#2 is supposed to show cemented intervals. EF#4 and #5 are both shaly sandstones, however differs by diverse GR reading (60-65 API versus 53-60 API respectively). EF#6 and EF#7 electrofacies very close on both cross-plots but vary by average porosity and GR reading range (20% versus 21% Porosity and 45-52 API versus 40-46 API respectively). EF#8 correspond to sandstones with some shale content, while EF#9 electrofacies represent clean sandstones. EF#10 shows data points from the best porosity (in average 30%) clean sandstones. Unlike in unsupervised electrofacies model, which contains only two high porosity (>25%) sandstone electrofacies, EF#11 and EF#12, supervised model separated these sandstones into three electrofacies, EF#8, EF#9, EF#10.

In the facies table on Figure 23 column 'Facies' demonstrates correspondence of electrofacies to core facies. Contingency table on Figure 24 shows model facies probabilities of correlating with a core facies. RHOB-NP and DNS-GR cross-plots, shown at Figure 25, from unsupervised electrofacies modelling (yellow background cross-plots) and supervised one (blue background cross-plots) illustrate dramatic decrease in modelling data volume.

	NAME	COL	PAT	WEIGHT	DENS	DNS	NEUT	GR	FACIES 1 2 3 4 5 6 7 8	OK4MODEL
1	Offshore_Shales			64						
2	Cemented			5						
3	Shaly_SS			9						
4	Sh_SS_60<GR<65			26						
5	Sh_SS_53<GR<60			17						
6	SS_Poro20_45<GR<52			8						
7	SS_Poro21_40<GR<46			14						
8	Sh_SS_25<Poro<28			16						
9	Clean_SS_25<Poro<29			16						
10	Clean_SS_Poro30			6						

Figure 23: Supervised facies table

Model Facies Probabilities (Reconstruction Rates)

MRGC_13_CLUST_FINAL

CORE_FACIES_ISS_HR_FACIES	Offshore_Shales	Cemented	Shaly_SS	Sh_SS_60<GR<65	Sh_SS_53<GR<60	SS_Poro20_45<GR<52	SS_Poro21_40<GR<46	Sh_SS_25<Poro<28	Clean_SS_25<Poro<29	Clean_SS_Poro30	TOTAL
2	30%	50%	10%			10%					100%
3								50%	50%		100%
5	56%		7%	24%	13%						100%
6					33%			67%			100%
7						10%	17%	37%	37%		100%
8					7%	15%	33%	7%	15%	22%	100%

Figure 24: Contingency table of core facies and modelled electrofacies. Probability of a core facies corresponding to each electrofacies is calculated. Dark blue colour is the least probable, while bright green is the most probable occurrence.

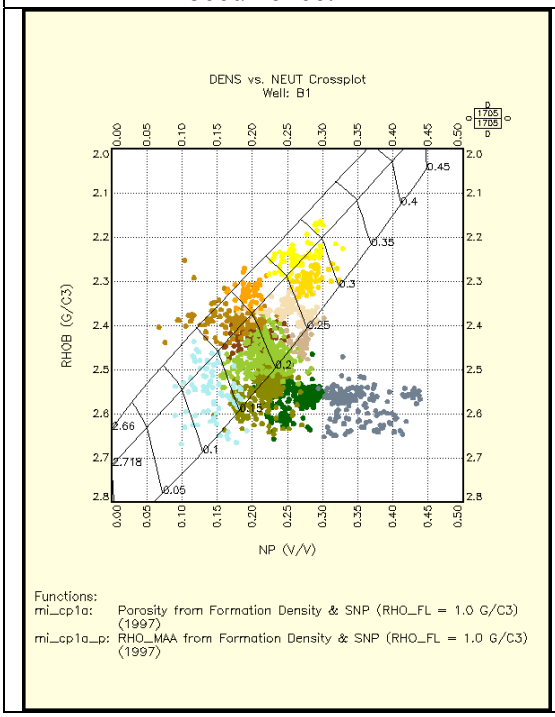

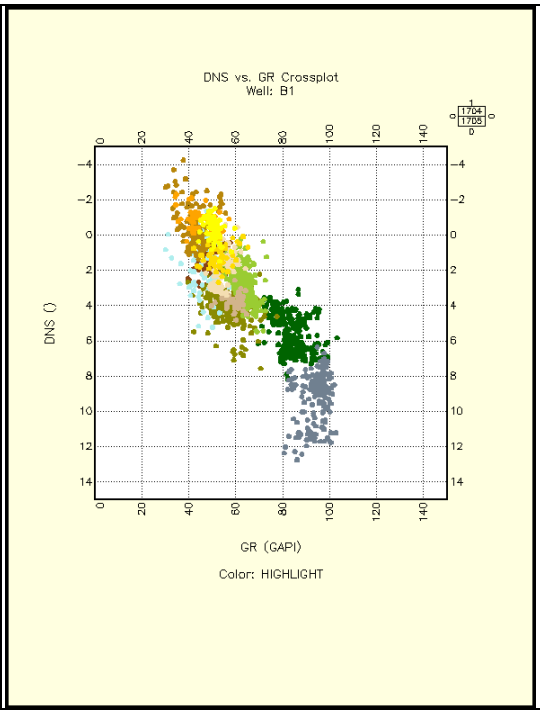

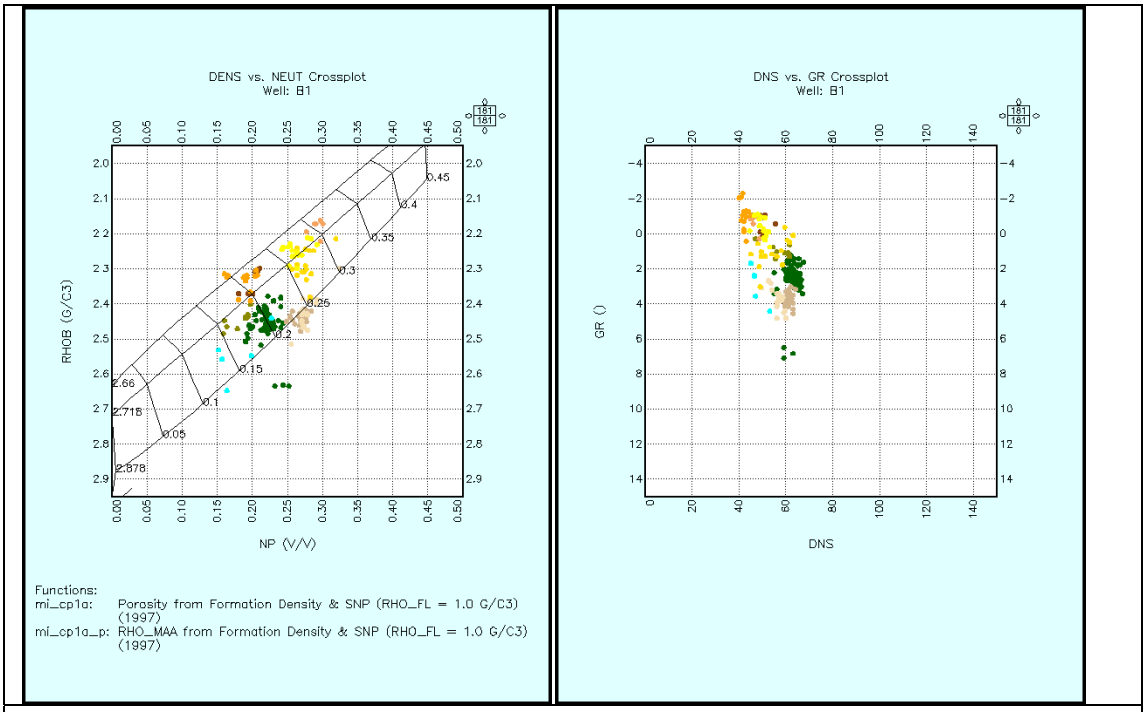

Figure 25: Final electrofacies distributed in RHOB-NP (left) and DNS-GR (right) cross-plots. Yellow background cross-plots are related to unsupervised modelling, blue background cross-plots represent supervised modelling.

3.1.3 QC OF UNSUPERVISED AND SUPERVISED MODELS

Comparison between the supervised and unsupervised models, together with the internal Cook layering and sedimentary environments is summarized in Table 6. As seen from the table, supervised model gives an advantage in high porosity sands within 3f layer of Cook 4, however, it does not recognise different types of shaly sandstones and shales, and overestimates cementation, particularly in Cook 1 layer. Unsupervised model reflects heterogeneity, identifies cemented intervals clearly, and distinguishes shale types. Besides the existence of minor uncertainties as identified in the unsupervised model, it still remains the most adequate model to be propagated across all the wells used in this study.

Finally, 12-electrofacies unsupervised model shows good coherence with core facies, sedimentary environment, and layering as defined by TEPN. Therefore, this model is chosen as the key reference electrofacies model for the propagation to the rest of the wells used in this study.

Table 6: Comparison of unsupervised and supervised electrofacies models in terms of identification capability.
EF# 1- EF#12 represent the electrofacies numbers,
Cell colour infers to:

- Green – good model correspondence (✓).
- Yellow – moderately sufficient correspondence
- Red – misleading model correspondence

Formation	Layer or general composition	Key QC intervals identification	Unsupervised model	Supervised model
Cook 7	6a, 6b, 6c	Three different depositional environment	✓	✓
		Cemented interval	EF#4	EF#2
		Specific electrofacies representation of the Intra-Cook offshore shales	EF#5	EF#1
Cook 6	5b	Heterogeneity	EF#7, EF#10	EF#7, EF#6
	5a	Heterogeneity	Some	Some
Cook 5	4b	Extensive x-bed unit	EF#9, EF#11, EF#12	EF#5, EF#8
		Cemented interval	EF#4	EF#2
	4a	Heterogeneity	✓	✓
Cook 4	3f	Heterogeneity	✓	Better recognition
		Negative DNS body separated	Less accurate picking of the body	Accurately picked
	3e	Heterogeneity	✓	✓
	3d	Separated upper most and lower most part of the layer with positive DNS	EF#9 identifies shaly sandstones with porosity approximately 20%	EF#1, which usually represent shaly low porosity zones
		Separated intermediate part with negative DNS	EF#7	EF#6, EF#8
Cook 3	3c	Cemented interval	Slightly wider range	Accurately picked
		Heterogeneity	✓	Partly
	3b	Heterogeneity	✓	✓
		Cemented interval	✓	Too wide cemented interval
	3a	Heterogeneity	EF#5 with a strike of EF#9, showing thin sandy layer	EF#1, no heterogeneity picked
Cook 2	2c	Heterogeneity	Partly	Partly
		Cemented interval	EF#4	EF#2
	2b	Heterogeneity	Generally good picking	Generally good picking
		Cemented interval	EF#4	EF#2
	2a	Offshore shales	✓	✓

Cook 1	1d	Upper body with low GR reading separated from lower one	Accurately picked	Shown only by one strike, cementation is overestimated
	1c	Upper body low GR separated from lower one	Accurately picked	Shown, cementation is overestimated
	1b	Cemented interval	EF#4	EF#2
		Heterogeneity	Partly	Shown, cementation is overestimated
	1a	Cook offshore: the same facies for Cook offshore as in Upper Cook?	EF#5 appears as a strike, but EF#3 prevails	Shaly zone is shown by EF#1, which usually represent marine offshore shales
		Cemented interval	EF#4	EF#2

3.2 Propagation of key electrofacies model

The unsupervised Well B1-based electrofacies model is propagated to the seven wells used in this study. High porosity sandstones have been revealed within the Cook sandstones by EF#9-12. Well B3 has extremely high porosity (30-35%) sandstones, and are also recognized as EF#12. The cemented intervals are accurately picked by the model in A and B prospect wells, however, they seem to be overestimated in D2 and D3 prospect wells.

Cook sandstones are known to be highly heterogeneous in facies (TEPN – Well B1 Confidential Report, 2014), and this is detected by the propagated model. The intra shales within the Cook sandstones are clearly identified in most of the wells as key lithological boundaries that correspond to EF#2, EF#3 and EF#5.

The non-coherence observed especially in cemented zones within the D prospect wells might be related to a possible change in mineralogical composition of the sediments as described in mudlog reports (TEPN – Confidential Report, D Field, 2010).

3.3 Correlation

During this study, the propagated electrofacies model allows for additional calibration of the formation tops initially picked by TEPN

Below in Figure 26 and Figure 27 is a display of two maps; West-East and North-South trending cross-sections respectively:

West-East cross-section is taken from the prospect A to B and passes through all wells drilled in these prospects (wells A1, A2, B3, B1, and B2), and is represented on Figure 26;

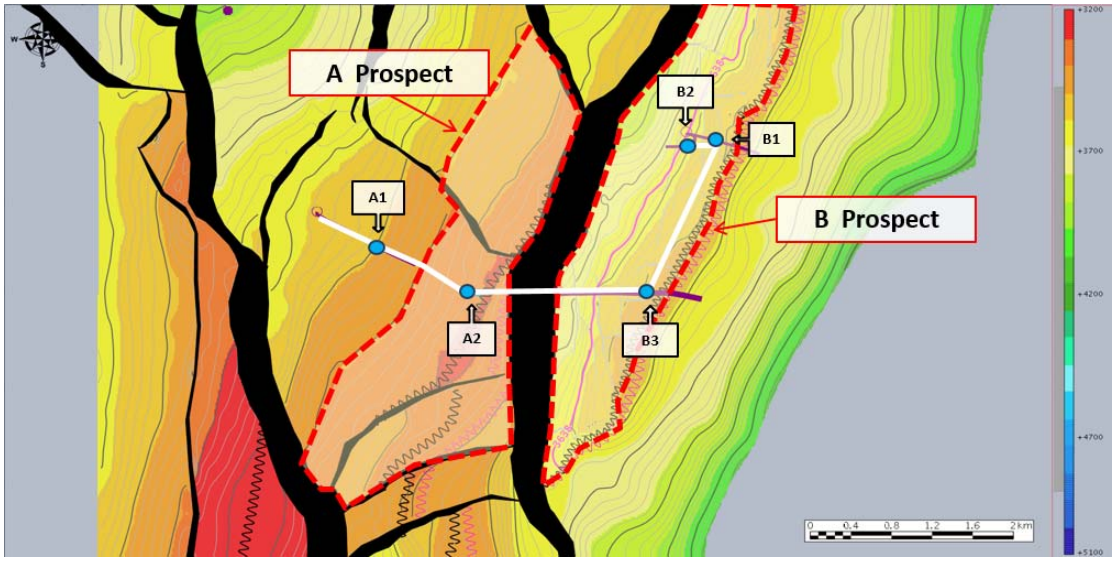

Figure 26: Map of A and B prospects (red dashed polygons), location of wells (blue points) included into West-East cross-section, shown as white solid line.

North-South cross-section extends from the prospect D to B and passes through the three wells drilled in prospect D as well as the two wells drilled in prospect B (wells D1, D2, D3, B1, and B3), is shown on Figure 27.

Existence of the electrofacies model in the wells provides the following results:

1. Internal layering as defined within TEPN was optimised and adjusted where necessary;
2. Internal layering for well D1 was not established prior to this study but this has now been defined using the electrofacies model as a basis for correlation;

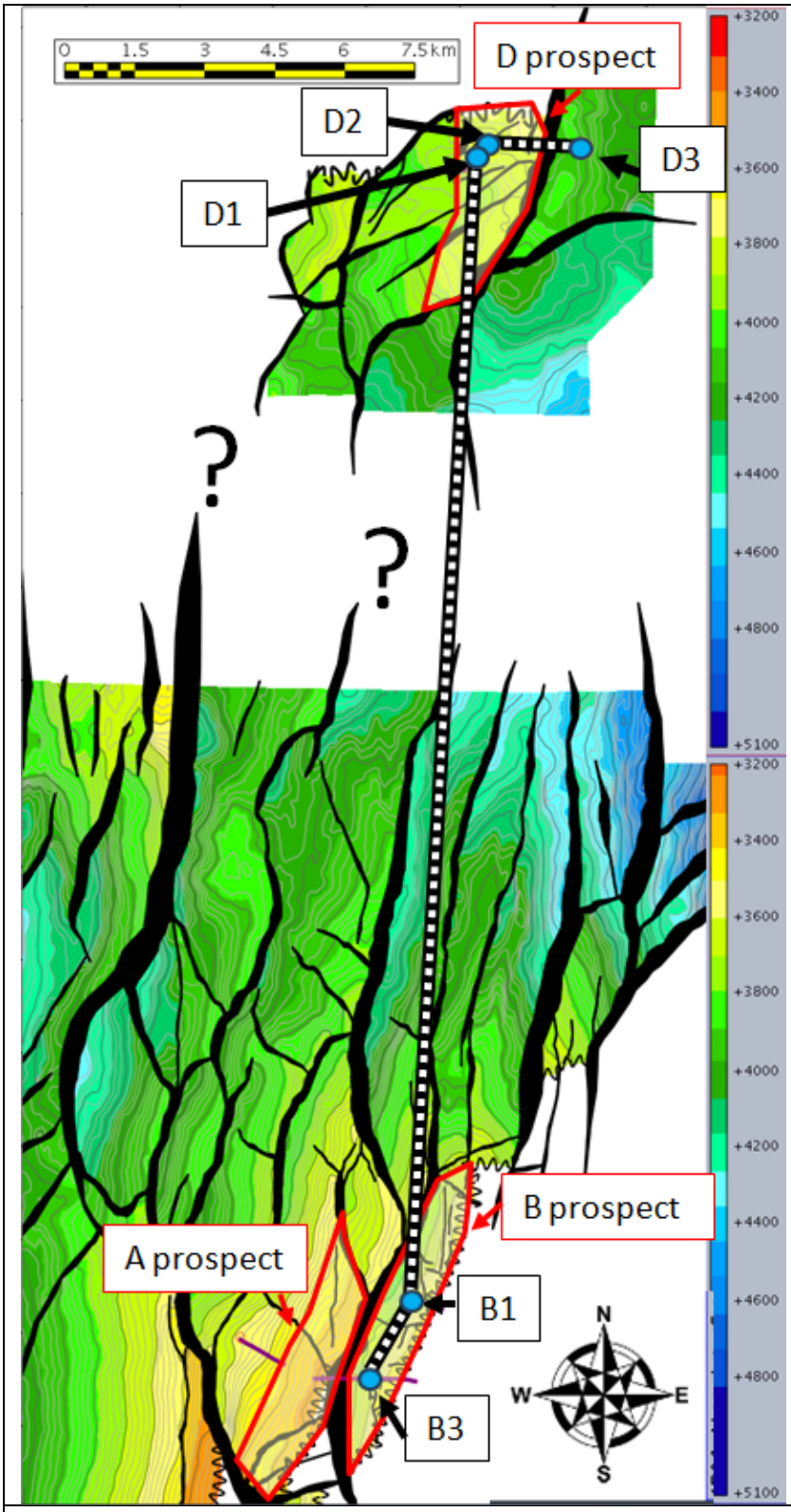

Figure 27: Map of A, B and D prospects (red solid polygons), location of wells (blue points) included into North-South cross-section, shown as white dashed line.

3. True stratigraphic thickness (TST) has been revised based on refined boundaries;
4. Cemented zones are properly captured within an assigned facies;
5. The Cook Formation based on electrofacies grouping done as seen. The propagated model has been used to separate the shoreface interval at the top from the basal estuarine and tidal influenced zones. Hence, the Cook formation can be grouped on this basis into Upper and Lower Cook interval respectively as seen in Table 7.

Table 7: Cook layering

COOK	Layer
Upper Cook	7
	6
	5
Lower Cook	4
	3
	2
	1

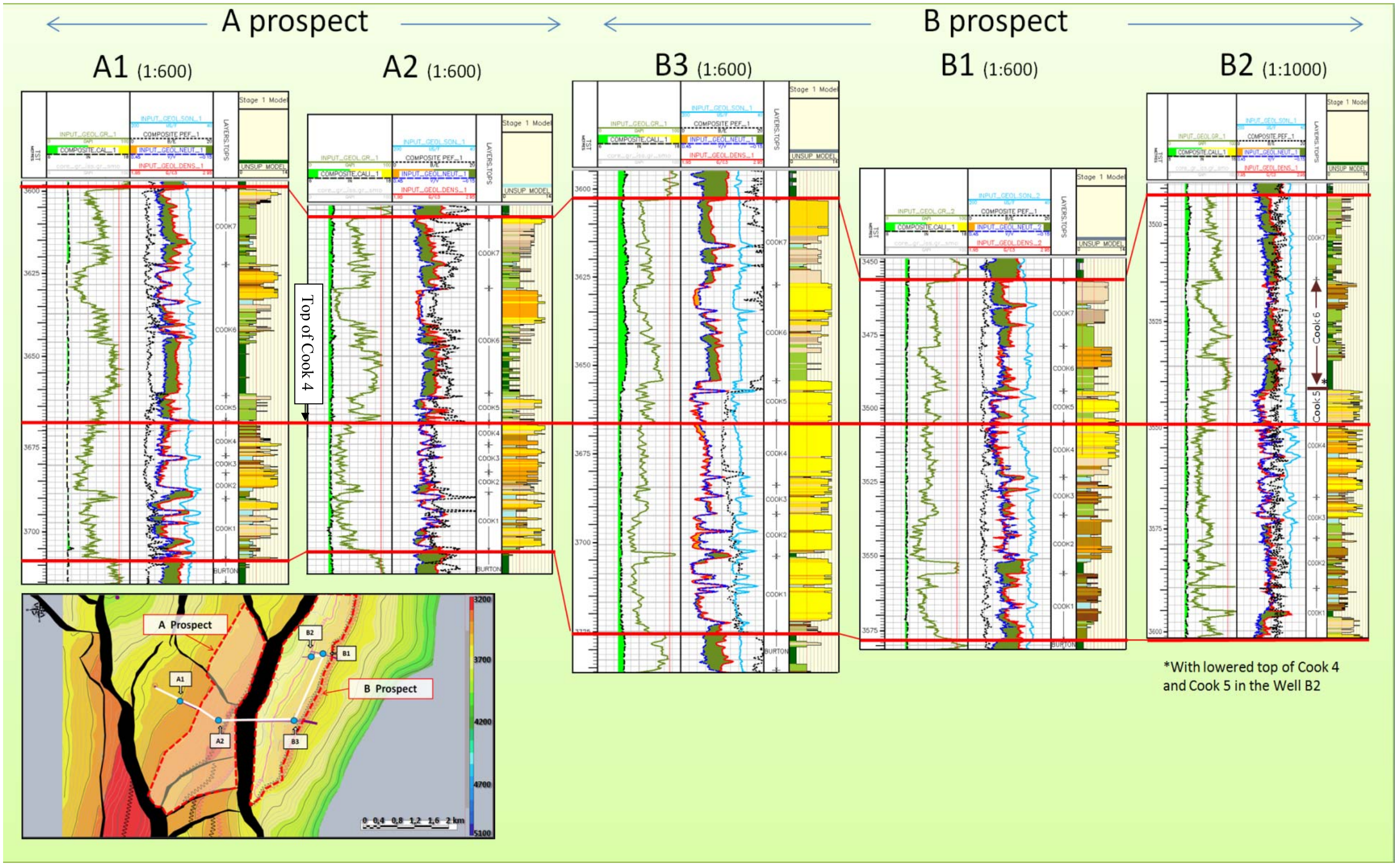

Figure 28: West-East trending cross-section through A1, A2, B3, B1 and B2 wells, flattened on top of Cook 4, and map, showing well location. The first track to the seventh are TST (m), GR (0-100 API), SON (200-40 US/F)-PEF (0-20 B/E)-NP (0,45-(-0,15) V/V)-RHOB (1,95-2,95 G/C^3), formation layering, Well B1-based electrofacies log;

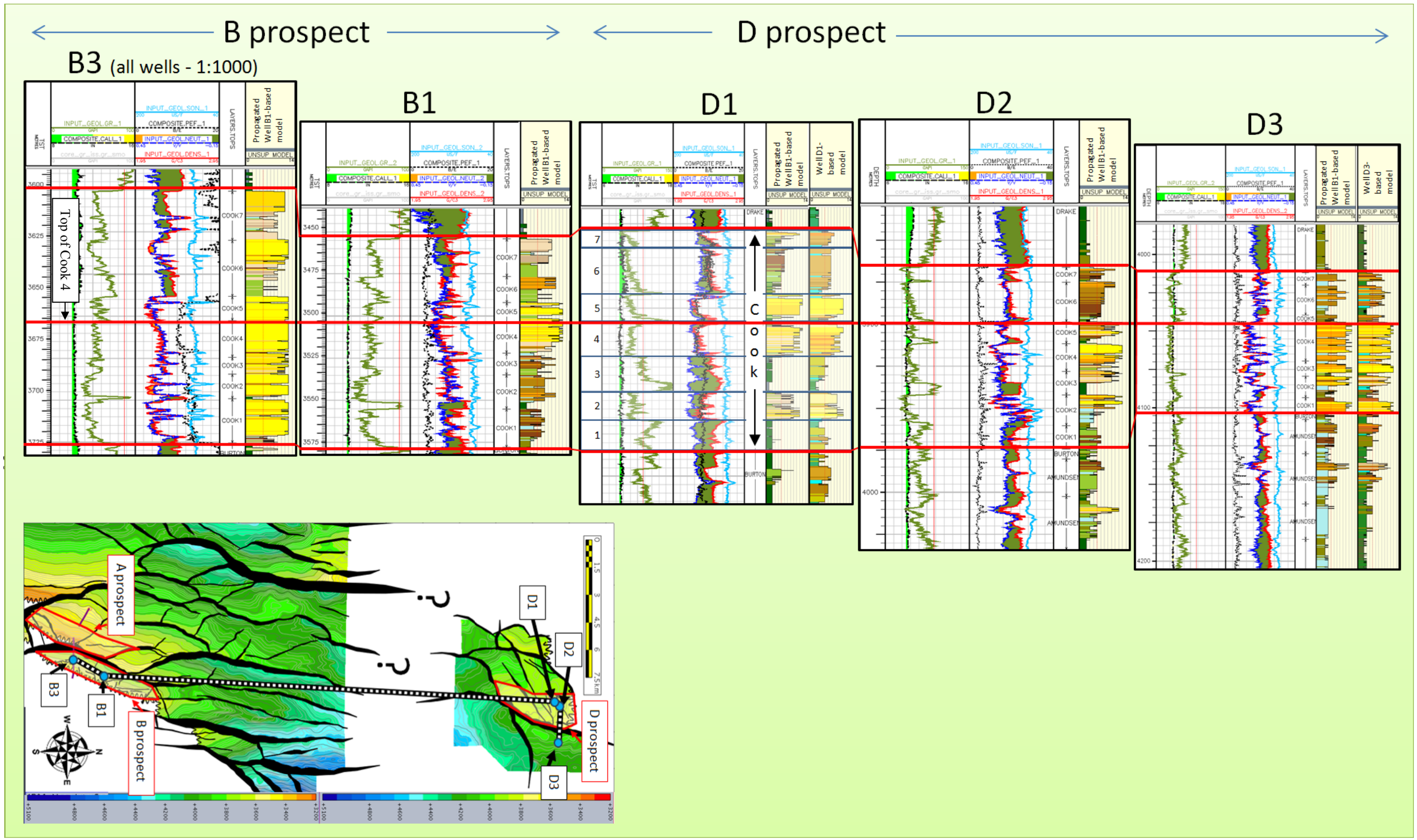

Figure 29: North-South trending cross-section through B3, B1, D1, D2 and D3 wells, flattened on top of Cook 4, and map, showing well location. The first track to the fifth are TST (m), GR (0-100 API), SON (200-40 US/F)-PEF (0-20 B/E)-NP (0,45-(-0,15) V/V)-RHOB (1,95-2,95 G/C^3), formation layering, Well B1-based electrofacies log, local well-based electrofacies log (in Wells D1 and D3);

4. PALEOGEOGRAPHICAL RECONSTRUCTION USING ELECTROFACIES MODEL

Internal studies of the depositional environment as carried out by TEPN are based mainly on cores and image logs of wells B1 and B3 (TEPN – Well B1 Confidential Report, 2014; – Well B3 Confidential Report, 2015). A possible modern analogue of the Cook environment is chosen at the North Sea coast of northern Germany and south-eastern Denmark (Figure 30). It is assumed that Lower Cook was accumulated in tide-dominated estuarine settings, while the Upper Cook was deposited in barrier lagoon, foreshore and shoreface settings (TEPN – Well B1 Confidential Report, 2014). The selected coastline is believed can represent both Lower and Upper Cook depositional environment. **Error! Reference source not found.** shows a possible analogue for the depositional environment for both Upper and Lower Cook in well B1

Lower Cook: tide-dominated estuary

Tide-dominated estuary is characterized by both estuarine and tidal influenced areas, which comprise channel, bar, and sandflat bodies (Figure 31 and Figure 32). According to the sedimentary facies derived in Wells B1 and B3, Well B1 is located in more estuarine settings, while Well B3 has penetrated more tidal high energy deposits. Based on the depositional environments and electrofacies calibrated to them, 3-dimensional depositional environment model has been created (Figure 33). The depositional environment model represents Lower Cook and its electrofacies associations linked together by their depositional environment.

Upper Cook: barrier-lagoon system, foreshore and shoreface

This environment involves large tide-dominated lagoon and foreshore, shoreface settings as observed in Cook 6 and Cook 7. It is assumed, Well B1 comprise sediments accumulated in a less dynamic environment rather than those of Well B3.

Assumed location of wells is shown on modern analogue on Figure 34. The 3-dimensional depositional environment model, represented on Figure 35, illustrates correspondence families of electrofacies to depositional elements. Wells B1 and B3 are placed on the model according to the sedimentary facies described from the cores.

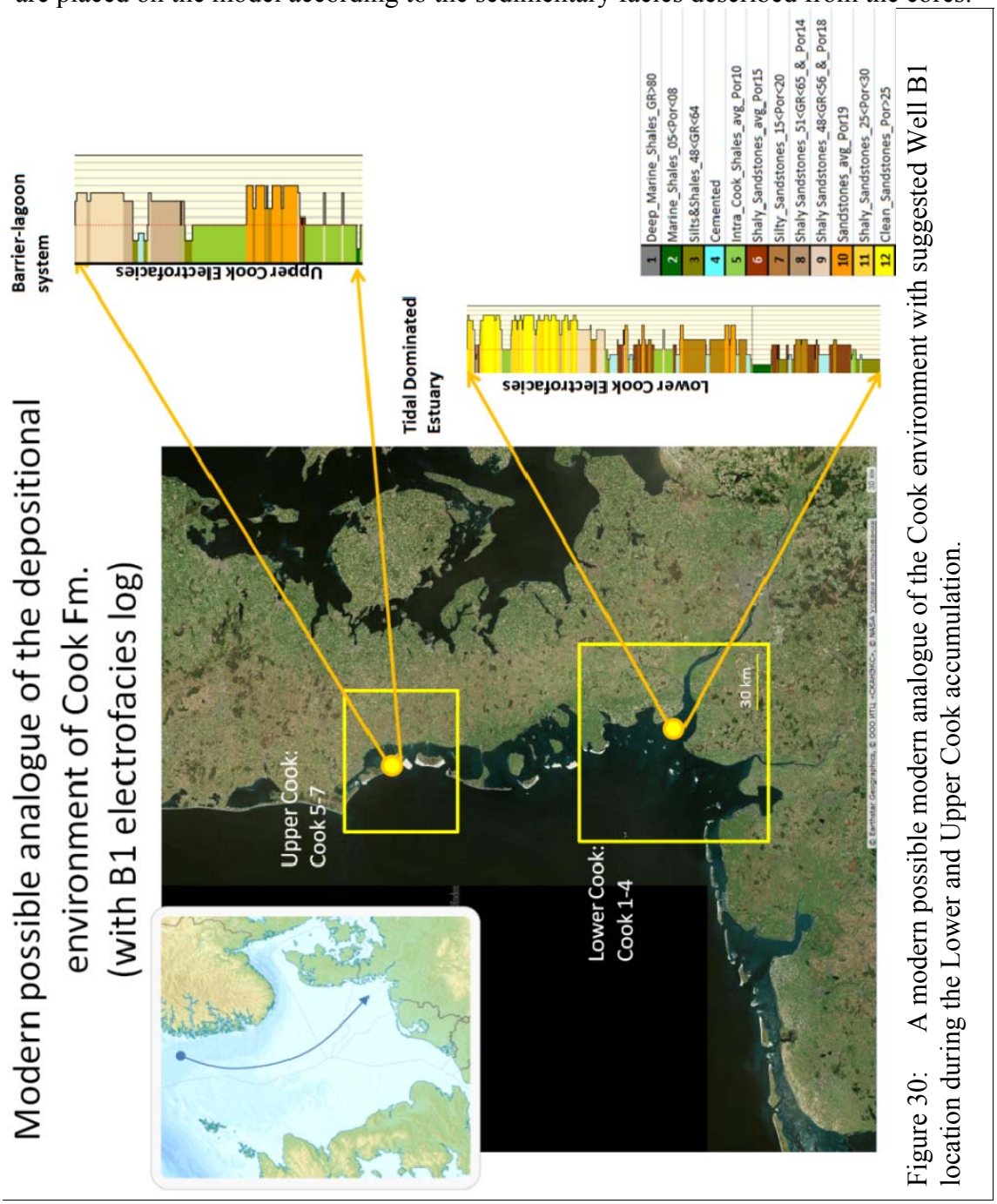

Figure 30: A modern possible modern analogue of the Cook environment with suggested Well B1 location during the Lower and Upper Cook accumulation.

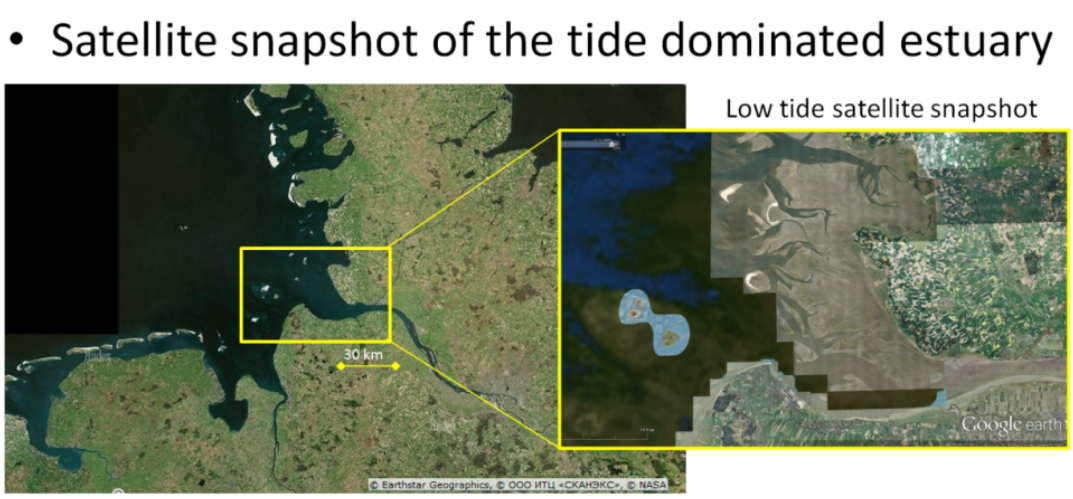

Figure 31: A modern analogue of the Lower Cook depositional environment: South-Eastern North Sea, German north-west coast.

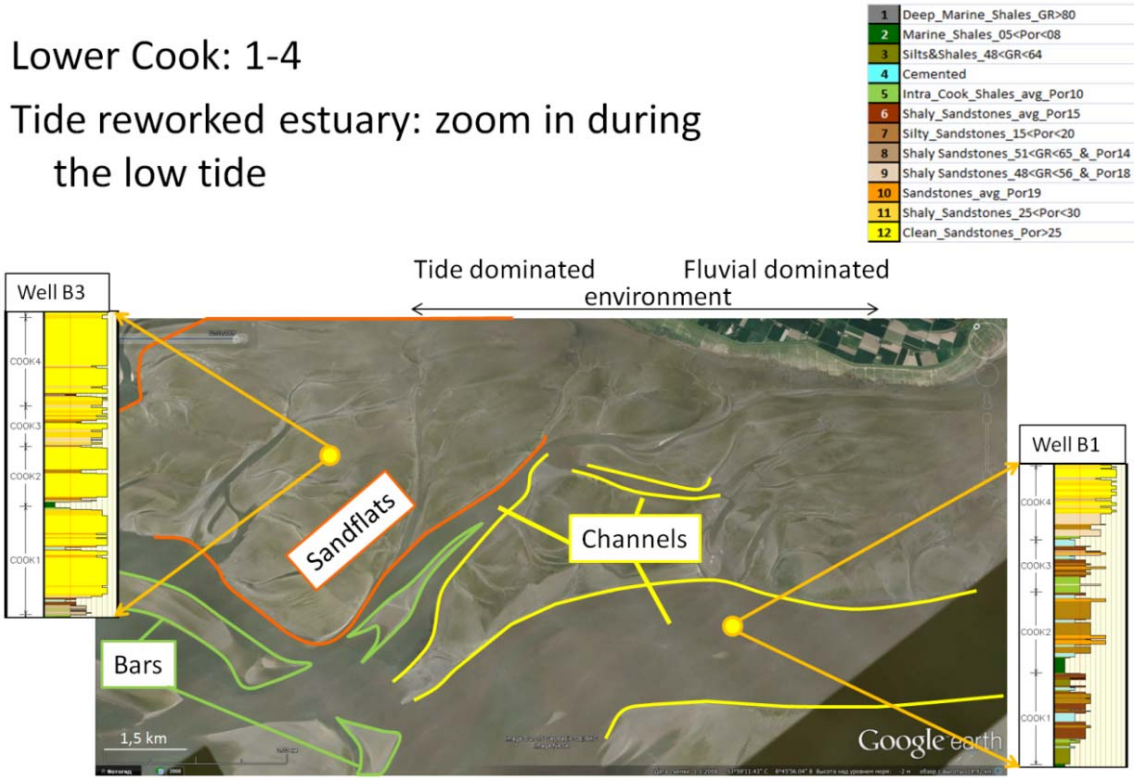

Figure 32: A modern analogue of the Lower Cook depositional environment with depositional elements. Well B1 is assumed has penetrated relatively fluvial dominated deposits, while Well B3 is believed has penetrated rather tide influenced deposits.

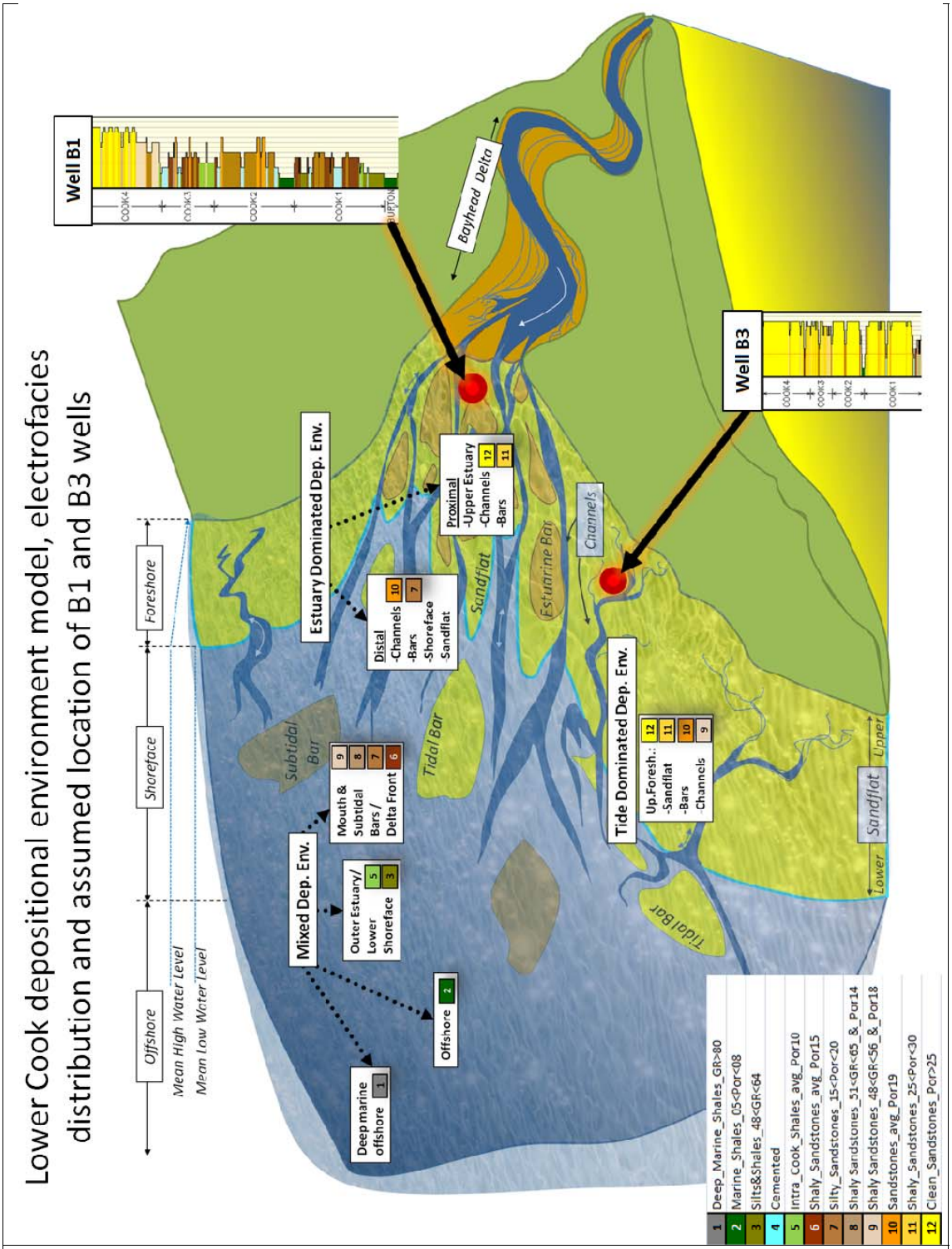

Figure 33: 3-dimensional depositional environment model of the Lower Cook with Well B1 and B3 location, and distribution of electrofacies associations related to the environment.

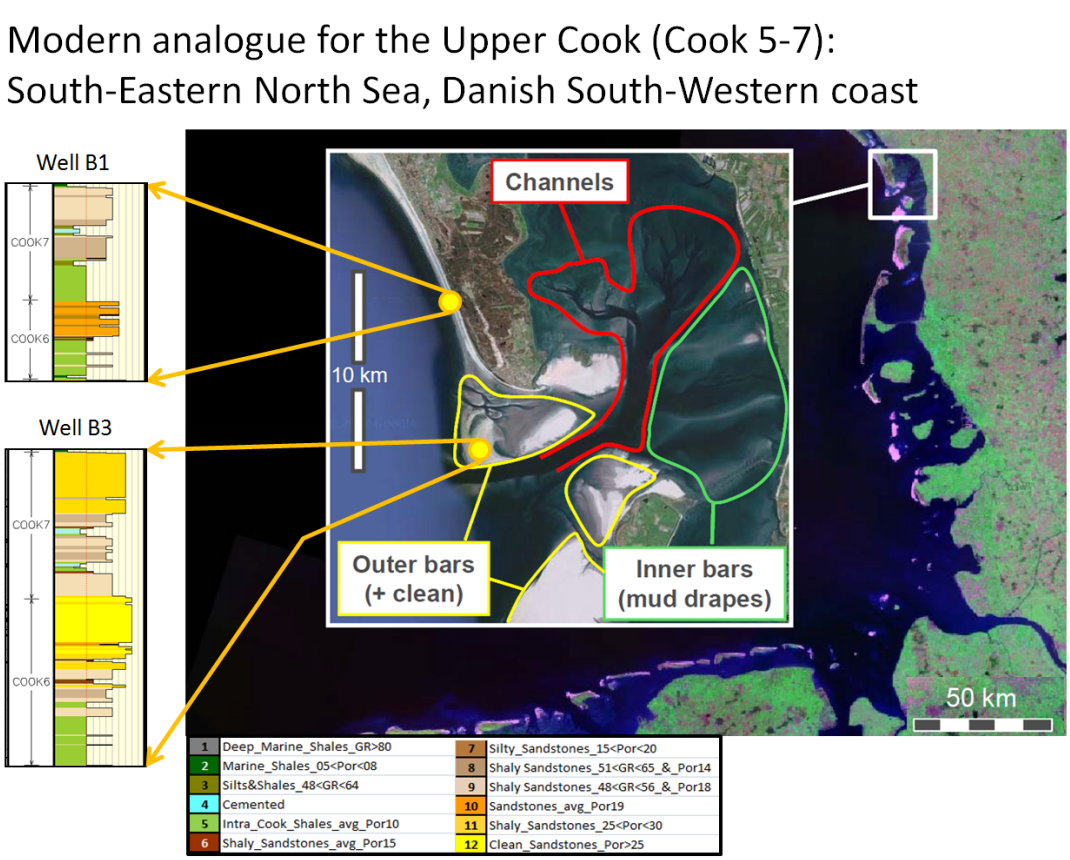

Figure 34: A modern analogue of the Upper Cook depositional environment with depositional elements. Well B1 is assumed has penetrated relatively open marine deposits, while Well B3 is believed has drilled into the deposits accumulated in higher energy environment.

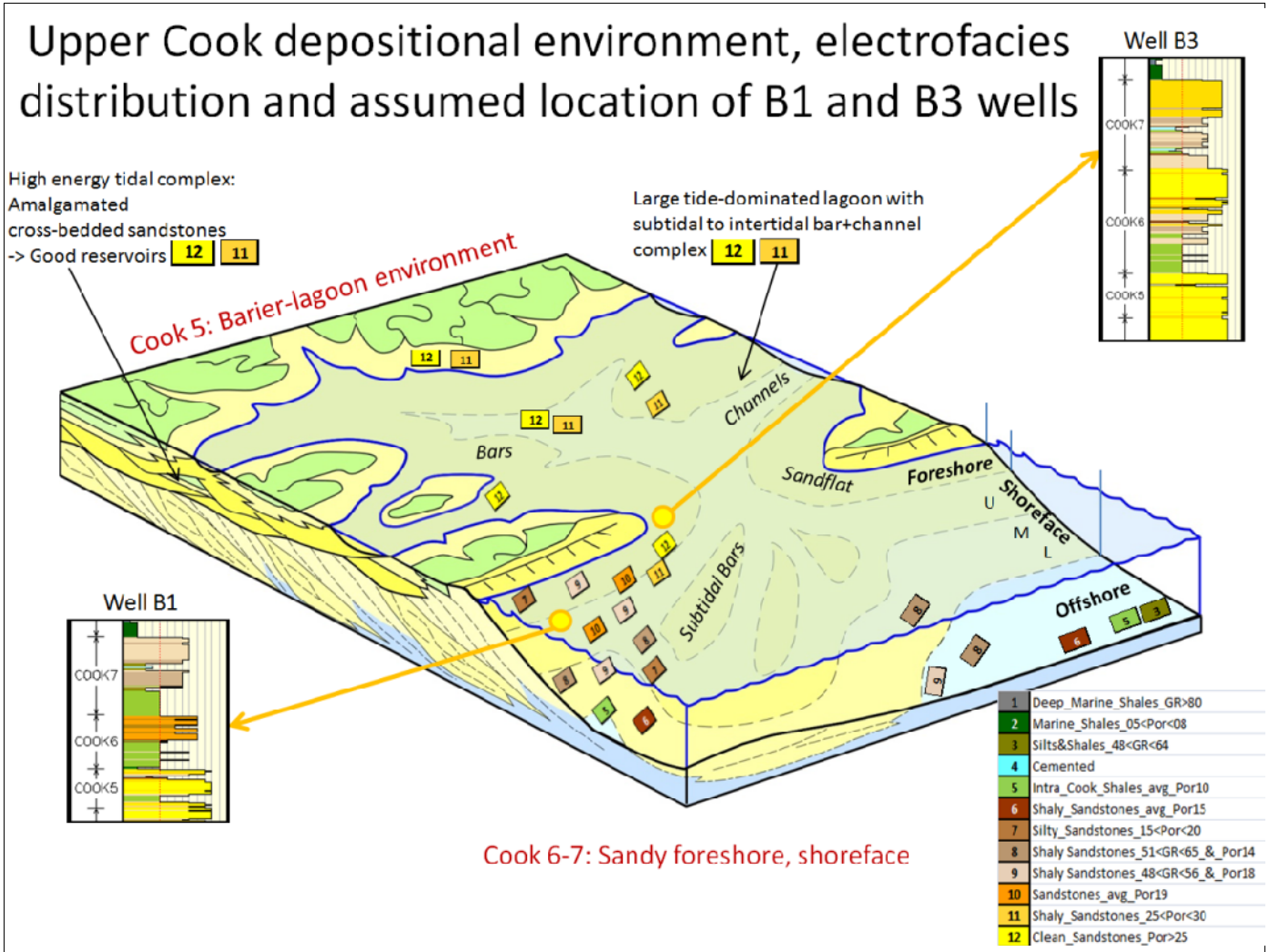

Figure 35: : 3-dimensional depositional environment model of the Upper Cook with Well B1 and B3 location, and distribution of electrofacies associations related to the environment (modified after TEPN – Well B1 Confidential Report, 2014).

5 PALEOGEOGRAPHY MODEL PROPAGATION OVER THE OTHER WELLS

3-dimensional depositional environment models and associated electrofacies families are used for prediction of the Cook paleogeography for A and B prospects. Prospect D is noted by mineralogical distinction (TEPN – Confidential Report, D Field, 2010), and therefore, prediction of paleogeography is highly uncertain.

Figure 36 represents predicted depositional settings of the Lower Cook in the area of A and B prospects.

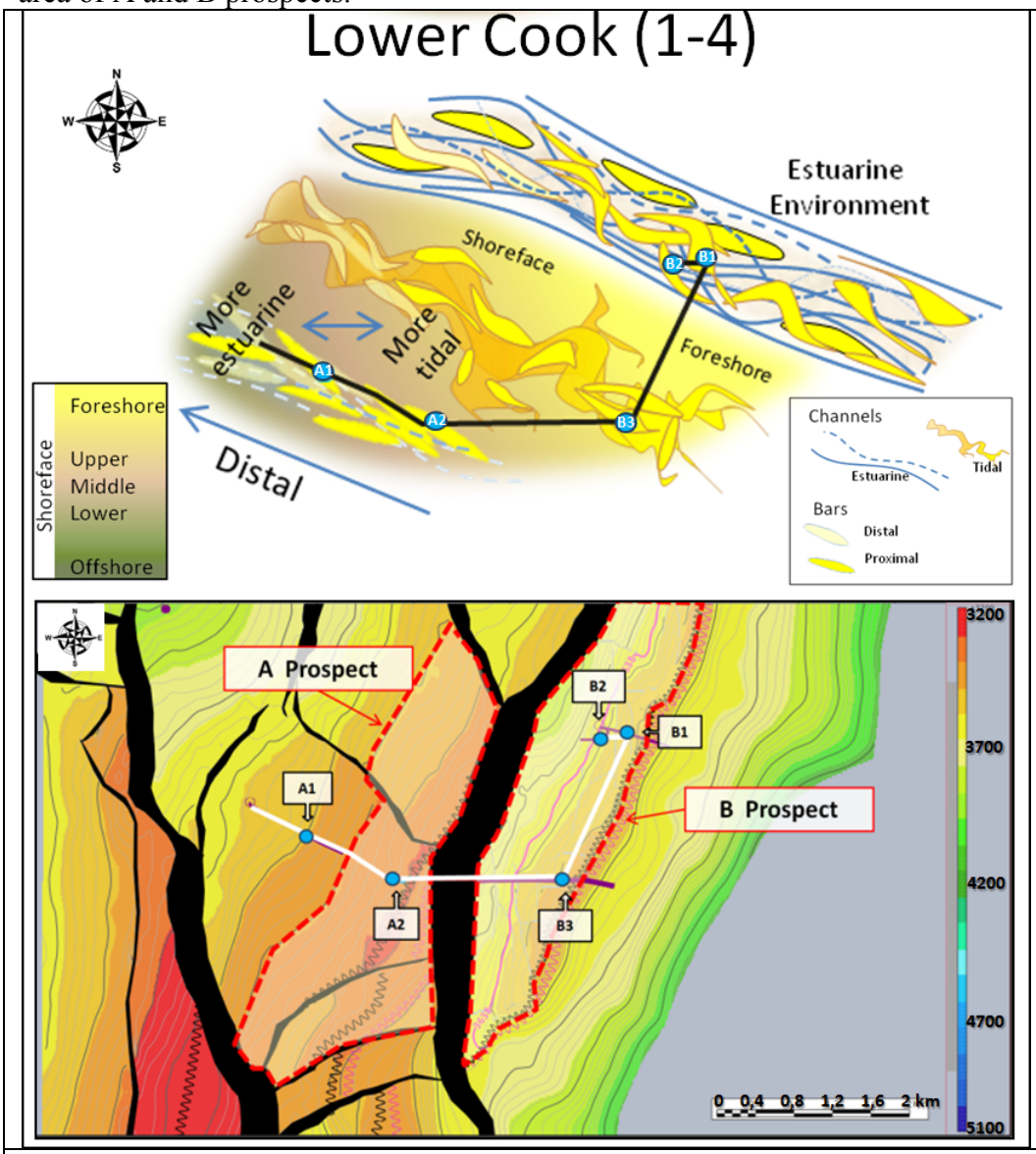

Figure 36: Interpreted paleogeography of A and B prospects during the Lower Cook.

Tide dominated area in the centre is bounded by estuarine belts with WNW flow direction. Well A1is located in a distal estuarine environment slightly influenced by tides. Well A3 is situated in mixed estuarine and distal tidal settings. Well B3 is the most proximally located well in foreshore and upper shoreface settings with associated stacked tidal channels and bars.

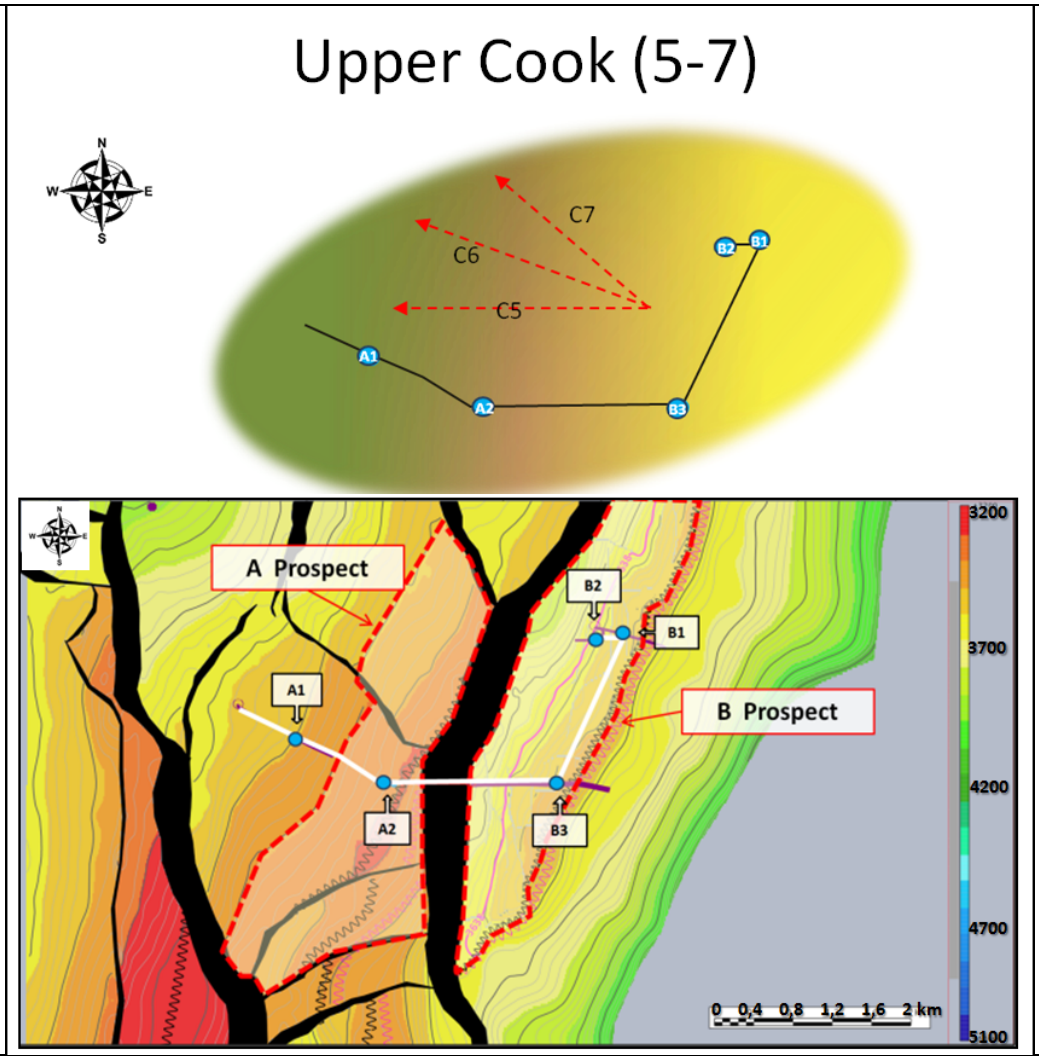

Figure 37: Interpreted paleogeography of A and B prospects during the Upper Cook. C5-C7 are degradation trends for Cook 5, Cook 6 and Cook 7 respectively.

Figure 37 illustrates Upper Cook depositional environment reconstructed for A and B prospects. It is believed that Cook 5 – Cook 7 are comprised by three backstepping wedges (TEPN – Well B1 Confidential Report, 2014), accumulated in shoreface and

foreshore homogeneous environment. Electrofacies analysis detected rotation of the degradation trend from E-W at Cook 5 to SE-NW at Cook 7 (Figure 37).

6 BLIND TEST ON WELL B3

A quick blind test at the end of the study was run on Well B3. The resulting Blind test model is compared with the reference electrofacies model. Basic input logs using GR, Density, Neutron Porosity, Sonic, DNS, Resistivity have also been used as input for the Blind test model (Figure 38 and Figure 39).

In general, Well B3 is seen to be sandier with less mud drapes, well sorted sands of higher porosity (30-35%) when compared the key Well B1. The porosity and grain size from the core samples taken in the Lower Cook interval of Well B3 also confirms this observation

Due to absence of these extreme high porosity sands (between 30-35%), the propagated reference electrofacies model, when compared to the blind test model tends to cluster all sands above 25% as one unit assigned to a specific electrofacies. Hence the >30% porosity sands are not distinguished as a separate electrofacies layers (Figure 40). The core facies from the well B3 is also consistent with the result using the propagated model as seen on Table 8.

#	Name	COL	PAT	WEIGHT	DENS	DNS	GR	NEUT	RDEEP	SON
1	Deep_Marine_Shales_GR>80			331						
2	Marine_Shales_+4<DNS<+8			252						
3	Cemented			59						
4	Intra_Cook_Offshore_Sh_Ss			753						
5	Clean_Sandstones_17<Por<27_-2<DNS<0			220						
6	Clean_Sandstones_20<Por<25_0<DNS<+2			50						
7	Silty_Sandstones_27<Por<30			75						
8	Sh_SS_Drake_32<Por<37			31						
9	Sandstones_25<Por<30_-4<DNS<+1			189						
10	Sandstones_30<Por<35_0<DNS<2			85						
11	Sandstones_30<Por<35_-4<DNS<0			114						
12	Sandstones_32<Por<35_-2<DNS<0			96						
13	Sandstones_35<Por			42						

Figure 38: Final facies table of the electrofacies model, based on Well B3 data, and log characterization of each electrofacies.

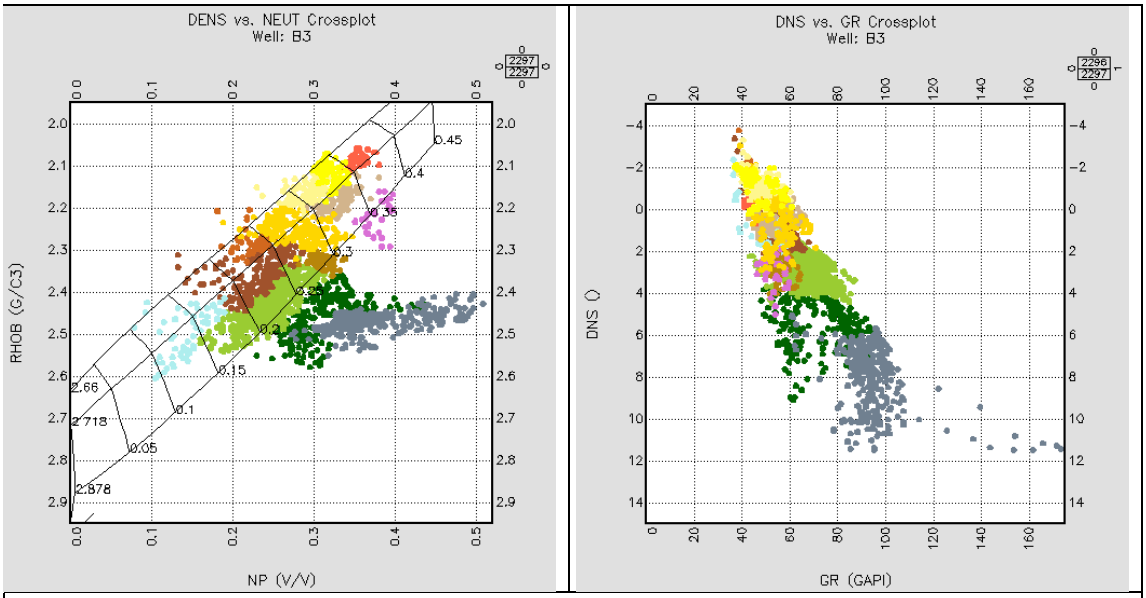

Figure 39: Final electrofacies of Well B3-based unsupervised model, distributed in RHOB-NP (left) and DNS-GR (right) cross-plots.

The most significant cemented intervals are accurately shown on both of the electrofacies models. Shaly intervals such as Intra-Cook shales as well as marine shales of Drake are well recognised by both models, while unsupervised B3 based electrofacies model underestimates Drake sandy interval.

Table 8 displays comparison of propagated model, Blind test Electrofacies from B3 and the core facies from well B3. The cored interval in well B3 has been cut in the most porous sandstones as seen in the Lower Cook Formation. The sandy core facies corresponds mainly to highly porous sandstones, particularly to EF#9-12 of propagated model and to EF#9-13 of the blind test model. Core facies representing cemented intervals correlates with EF#3 and EF#4 as seen in the propagated electrofacies model and the blind test model respectively.

Finally, comparison of the propagated electrofacies model and model based on Well B3 data shows that the first model is suitable both for less and more porous sediments in comparison to those of Well B1, with some heterogeneity neglected.

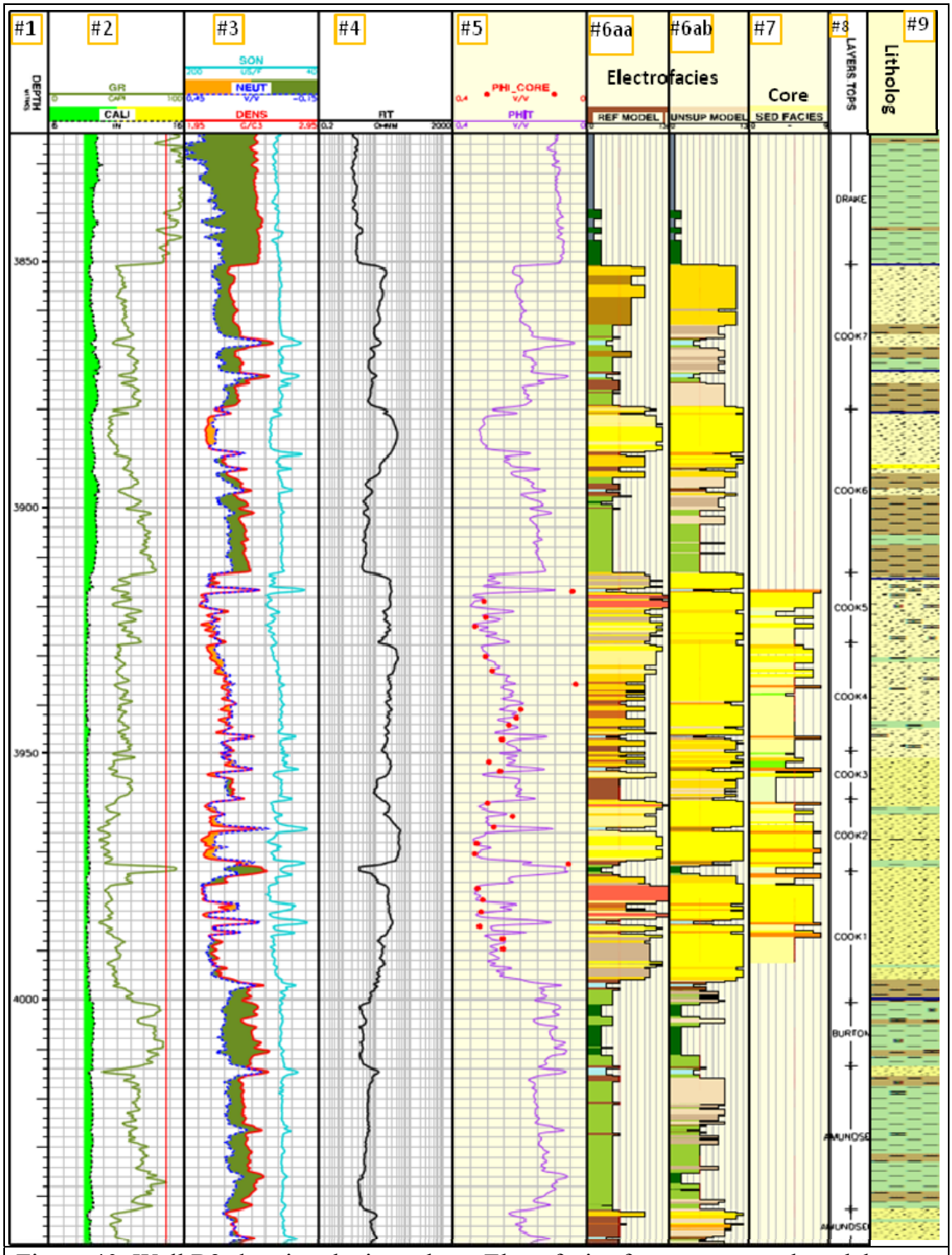

Figure 40: Well B3 showing the input logs; Electofacies from propagated model , Blind test Electrofacies from B3 and the core facies from well B3

Table 8: Core facies comparison with blind test model based on B3 and propagated electrofacies model from B1.

Core Facies	Description	Probability	Electrofacies # of Unsup.model based on Well B3	Electrofacies # of the propagated model based on Well B1
CF3	Shaly and sandy heterolithics, deposited in tide-dominated	All the e-facies	2, 4, 5, 6, 9, 10, 12	2, 7, 9, 11, 12
CF4	Horizontal to wavy-bedding sandstones with mud drapes and flakes, are interpreted as subtidal deposits in protected	Most likely	9	12
		Minor appearance	6	10
CF5	Cross-bedded well-sorted medium to fine sandstones with mud drapes, deposited in shallow subtidal to intertidal environment.	Most likely	9	9
			10	10
			11	11
			12	12
		Minor appearance	5, 6, 7	
CF6	Clean horizontal to wavy-bedding with mud drapes and flakes are deposits of a shallow coastal setting with permanent wave action, possibly in a tidal sand flat ro foreshore settings.	Most likely	11	11
			12	12
		Minor appearance	6, 9	
CF7	Clean sandstones with cross-bedding are deposited in foreshore of shallow tidal channel deposits.	Most likely	9	12
			10	10
			11	
			12	
			13	
CF8	Calcite cemented sandstones are distinctive calcite cemented	Most likely	3	4
		Mix		5, 6, 7, 9, 10, 12

7 DISCUSSION

Electrofacies model tied to depositional environment helps to predict sedimentary facies and paleogeographic understanding in prospects where deposits have similar mineralogical composition to the key well sediments. Complex depositional settings, characterized by several diverse sources of sediments, require additional information of the sedimentary facies, such as core or image log facies both in key well and other wells. Lack of the data, however, does not affect to the petrophysical characteristics prediction in uncored wells, which can be used in geological modelling of a prospect. An unsupervised electrofacies model build in any uncored well is capable to support propagated one.

Prediction of the paleogeography is highly uncertain in remote areas, which are particularly lithologically and mineralogically discrepant. Petrophysical properties are might be predicted with some uncertainty degree by additional use of local unsupervised electrofacies model and controlled by litholog data.

8 CONCLUSION

Twelve electrofacies have been indentified using the key well linking log responses to core data. There is a relation between electrofacies associations within and sedimentary environment of a specific geobody. However, it is not possible to directly relate an individual electrofacies to any particular depositional environment.

Electrofacies provide aid for correlation of formation and layer tops. An existing correlation purely made on log signatures has been revised based on resulting electrofacies.

The prograding lowermost Cook and the retrograding uppermost Cook are characterized by different electrofacies families, although they must represent similar water depth evolution, suggesting different depositional environment. This has been confirmed by sedimentological studies of the core, suggesting the Lower Cook to represent an estuarine setting, while the Upper Cook represents a barrier-lagoon setting. As a result, two paleogeographic models have been built as representative for two parts of Cook separately. Paleogeographic reconstructions are done for A and B prospects based on propagated electrofacies.

However, the electrofacies model has its limitations. When using the propagated electrofacies based on the key prospect B to prospect D, located at a distance of 25 km, inconsistencies are observed. This may be due to slightly different mineralogical contents due to different sand sources, which will influence the log responses and therefore, electrofacies. Local electrofacies model, calibrated to the core is suggested to be used in such cases.

APPENDIX

	NAME	COL	PAT	WEIGHT	DENS	MINIMUM	MAXIMUM	MEAN	STD DEV
1	Deep_Marine_Sh			191		2.47	2.65	2.57	0.03
2	Marine_Sh			284		2.46	2.66	2.56	0.03
3	Cook_Offshore_Silts_Sh			330		2.46	2.65	2.54	0.04
4	Ss_cemented			78		2.44	2.67	2.55	0.06
5	Cook_Offshore_Sh_Ss			295		2.37	2.54	2.47	0.03
6	Sh_Ss_Poro_15-22			108		2.38	2.47	2.43	0.02
7	Clean_SS_Poro_15-20			113		2.25	2.44	2 39	0.03
8	SS_Poro_20-25_F_Gr			46		2.38	2.47	2.44	0.02
9	SS_Poro_20-27_M-F_Gr			91		2.32	2.40	2.37	0.02
10	Clean_SS_Poro_20-25			56		2.27	2.36	2.32	0.02
11	SS_Poro_25-30			54		2.24	2.34	2.29	0.02
12	SS_Poro>25			59		2.16	2.29	2.24	0.03

Appendix 1: The minimum,maximum, mean and standard deviation details for Density Log for each electrofacies of key reference electrofacies model.

	NAME	COL	PAT	WEIGHT	DNS	MINIMUM	MAXIMUM	MEAN	STD DEV
1	Deep_Marine_Sh			191		6.35	12.75	9.25	1.45
2	Marine_Sh			284		3.09	8.18	5.68	1.04
3	Cook_Offshore_Silts_Sh			330		2.26	7.57	4.04	0.79
4	Ss_cemented			78		-1.37	5.22	1.75	1.49
5	Cook_Offshore_Sh_Ss			295		0.26	5.47	2.70	0.93
6	Sh_Ss_Poro_15-22			108		-0.34	3.11	1.47	0.65
7	Clean_SS_Poro_15-20			113		-5.47	1.38	-0 56	1.27
8	SS_Poro_20-25_F_Gr			46		2.57	4.83	3.77	0.41
9	SS_Poro_20-27_M-F_Gr			91		-0.54	3.46	1.95	0.91
10	Clean_SS_Poro_20-25			56		-2.31	0.33	-0.95	0.54
11	SS_Poro_25-30			54		0.11	2.73	1.24	0.56
12	SS_Poro>25			59		-1.47	1.48	-0.33	0.66

Appendix 2: The minimum,maximum, mean and standard deviation details for DNS Log for each electrofacies of key reference electrofacies model.

	NAME	COL	PAT	WEIGHT	GR	MINIMUM	MAXIMUM	MEAN	STD DEV
1	Deep_Marine_Sh			191		80.62	102.58	93.96	4.81
2	Marine_Sh			284		69.89	103.42	84.49	6.11
3	Cook_Offshore_Silts_Sh			330		39.75	77.65	56.60	5.78
4	Ss_cemented			78		30.40	57.18	46.67	5.52
5	Cook_Offshore_Sh_Ss			295		53.07	73.06	63.05	3.82
6	Sh_Ss_Poro_15-22			108		39.82	57.80	49.83	3.77
7	Clean_SS_Poro_15-20			113		30.22	55.55	43 03	5.21
8	SS_Poro_20-25_F_Gr			46		49.54	64.93	59.42	3.45
9	SS_Poro_20-27_M-F_Gr			91		46.04	64.32	54.54	3.84
10	Clean_SS_Poro_20-25			56		34.44	57.20	45.02	5.67
11	SS_Poro_25-30			54		42.32	65.12	52.63	4.79
12	SS_Poro>25			59		44.14	59.71	50.45	2.89

Appendix 3:The minimum,maximum, mean and standard deviation details for GR Log for each electrofacies of key reference electrofacies model.

	NAME	COL	PAT	WEIGHT	NEUT	MINIMUM	MAXIMUM	MEAN	STD DEV
1	Deep_Marine_Sh			191		0.29	0.44	0.35	0.04
2	Marine_Sh			284		0.20	0.30	0.25	0.03
3	Cook_Offshore_Silts_Sh			330		0.15	0.28	0.22	0.02
4	Ss_cemented			78		0.09	0.19	0.14	0.02
5	Cook_Offshore_Sh_Ss			295		0.16	0.28	0.22	0.02
6	Sh_Ss_Poro_15-22			108		0.16	0.25	0.21	0.02
7	Clean_SS_Poro_15-20			113		0.07	0.24	0 17	0.03
8	SS_Poro_20-25_F_Gr			46		0.25	0.30	0.27	0.01
9	SS_Poro_20-27_M-F_Gr			91		0.18	0.29	0.26	0.02
10	Clean_SS_Poro_20-25			56		0.16	0.22	0.20	0.01
11	SS_Poro_25-30			54		0.25	0.32	0.28	0.02
12	SS_Poro>25			59		0.22	0.33	0.27	0.02

Appendix 4: The minimum,maximum, mean and standard deviation details for Neutron Porosity Log for each electrofacies of key reference electrofacies model.

	NAME	COL	PAT	WEIGHT	SON	MINIMUM	MAXIMUM	MEAN	STD DEV
1	Deep_Marine_Sh			191		89.64	103.12	95.59	3.03
2	Marine_Sh			284		76.18	99.01	88.39	5.36
3	Cook_Offshore_Silts_Sh			330		66.19	86.42	80.17	3.12
4	Ss_cemented			78		62.96	83.76	73.43	4.84
5	Cook_Offshore_Sh_Ss			295		63.71	97.41	81.96	4.61
6	Sh_Ss_Poro_15-22			108		68.93	88.03	81.60	4.17
7	Clean_SS_Poro_15-20			113		65.77	88.16	78 56	4.30
8	SS_Poro_20-25_F_Gr			46		80.86	93.70	87.39	2.24
9	SS_Poro_20-27_M-F_Gr			91		77.10	94.30	86.49	3.28
10	Clean_SS_Poro_20-25			56		75.74	91.39	83.87	3.19
11	SS_Poro_25-30			54		82.39	103.96	93.33	5.06
12	SS_Poro>25			59		83.26	103.80	96.05	5.36

Appendix 5: The minimum,maximum, mean and standard deviation details for Sonic Log for each electrofacies of key reference electrofacies model.

	NAME	COL	PAT	WEIGHT	RDEEP	MINIMUM	MAXIMUM	MEAN	STD DEV
1	Deep_Marine_Sh			191		1.52	3.17	2.26	0.38
2	Marine_Sh			284		1.29	9.61	3.27	1.15
3	Cook_Offshore_Silts_Sh			330		3.14	40.81	5.21	4.15
4	Ss_cemented			78		3.69	107.31	20.57	20.44
5	Cook_Offshore_Sh_Ss			295		3.26	20.24	6.48	2.74
6	Sh_Ss_Poro_15-22			108		3.12	54.24	14.66	8.09
7	Clean_SS_Poro_15-20			113		5.06	74.90	30 34	15.04
8	SS_Poro_20-25_F_Gr			46		4.43	22.69	8.13	3.47
9	SS_Poro_20-27_M-F_Gr			91		4.89	39.60	13.38	4.98
10	Clean_SS_Poro_20-25			56		17.07	84.84	41.50	17.18
11	SS_Poro_25-30			54		7.27	28.63	15.61	4.90
12	SS_Poro>25			59		7.78	22.97	13.73	3.75

Appendix 6: The minimum,maximum, mean and standard deviation details for Resistivity Log for each electrofacies of key reference electrofacies model.

REFERENCES

Chamock, M. A., I. L. Kristiansen, A. Ryseth, and J. P. G. Fenton, 2001, Sequence Stratigraphy of the Lower Jurassic Dunlin Group, Northern North Sea, *in* J. M. Ole, and D. Tom, eds., Norwegian Petroleum Society Special Publications, v. Volume 10, Elsevier, p. 145-174.

Deegan, C. E., and B. J. Scull, 1977, A standard lithostratigraphic nomenclature for the Mesozoic of the central and northern North Sea: Northern North Sea Symposium 1997 Proceedings, p. 24.

Doveton, J. H., 1994, Geologic log analysis using computer methods: AAPG computer applications in geology, Tulsa, Okla, American Association of Petroleum Geologists.

Dreyer, T., and M. Wiig, 1995, Reservoir architecture of the cook formation on the gullfaks field based on sequence stratigraphic concepts, *in* V. L. F. E. P. J. R.J. Steel, and C. Mathieu, eds., Norwegian Petroleum Society Special Publications, v. Volume 5, Elsevier, p. 109-142.

Evans, D., C. Graham, A. Armour, and P. Bathurst, 2003, Millennium Atlas: Petroleum Geology of Central and Northern North Sea The Geological Society of London.

Folkestad, A., Z. Veselovsky, and P. Roberts, 2012, Utilising borehole image logs to interpret delta to estuarine system: A case study of the subsurface Lower Jurassic Cook Formation in the Norwegian northern North Sea: Marine and Petroleum Geology, v. 29, p. 255-275.

Gibbons, K. A., C. A. Jourdan, and J. Hesthammer, 2003, The Statfjord Field, Blocks 33/9, 33/12 Norwegian sector, Blocks 211/24, 211/25 UK sector, Northern North Sea, Geological Society Memoir, p. 335-353.

Gupta, R., and H. D. Johnson, 2001, Characterization of heterolithic deposits using electrofacies analysis in the tide-dominated Lower Jurassic Cook Formation (Gullfaks Field, offshore Norway): Petroleum Geoscience, v. 7, p. 321-330.

Kumar, B., and K. Mahendra, 2006, Electrofacies Classification – A Critical Approach, 6th International Conference & Exposition on Petroleum Geophysics "Kolkata 2006", Kolkata, Schlumberger Information Solutions, p. 822-825.

Livbjerg, F., and R. Mjos, 1989, The Cook Formation, an offshore sand ridge in the Oseberg area, northern North Sea. : J.D. Collinson (Editor), Correlation in Hydrocarbon Exploration. Graham and Trotman, London, p. 299-312.

Marjanac, T., 1995, Architecture and sequence stratigraphic perspectives of the dunlin group formations and proposal for new type- and reference-wells, Norwegian Petroleum Society Special Publications, p. 143-149,153-165.

Marjanac, T., and R. J. Steel, 1997, Dunlin Group sequence stratigraphy in the northern North Sea; a model for Cook Sandstone deposition: AAPG Bulletin, v. 81, p. 276-292.

Parkinson, D. N., and F. M. Hines, 1995, The lower jurassic of the north viking graben in the context of western european lower jurassic stratigraphy, Norwegian Petroleum Society Special Publications, p. 97-107.

Ramsin, E., B. N. Rami, and D. Kersey, 2009, Real-time Geology/Petrophysics in Complex Carbonate Reservoirs, Society of Petroleum Engineers.
Serra, O., and H. T. Abbott, 1982, The Contribution of Logging Data to Sedimentology and Stratigraphy.
Stinco, L. P., 2006, Core And Log Data Integration. The Key For Determining Electrofacies, Society of Petrophysicists and Well-Log Analysts.
Teh, W., G. P. Willhite, and J. H. Doveton, 2012, Improved Reservoir Characterization in the Ogallah Field using Petrophysical Classifiers within Electrofacies, Society of Petroleum Engineers.
Volleset, J., and A. G. Dore, 1984, A revised Triassic and Jurassic lithostratigraphic nomenclature for the Norwegian North Sea: Norwegian Petroleum Directorate Bulletin, v. 3, p. 53.
Vollset, J., and A. G. Doré, 1984, A Revised Triassic and Jurassic lithostratigraphic nomenclature for the Norwegian North Sea: NPD-bulletin (online), Stavanger, Oljedirektoratet.
Ye, S.-J., and P. Rabiller, 2000, A New Tool For Electro-Facies Analysis: Multi-Resolution Graph-Based Clustering, Society of Petrophysicists and Well-Log Analysts.
Ye, S., and P. Rabiller, 2001, MULTI-RESOLUTION GRAPH-BASED CLUSTERING, Halliburton Energy Services, Inc., Houston, TX (US), Elf Exploration Production (FR), p. 20.

OTHER INTERNAL SOURCES:

TEPN Internal Reports:

Norsk HYDRO Final Well C1 Report, 1992. C Field. Confidential
TEPN (Total Exploration and Production Norge AS) Internal Report by Eliassen, H., Kvernes, S., et al., 2013. New Structural understanding on the C Field, northern area. Confidential
TEPN Internal Geological End of Well Report by Hiksdal, A., et al., 2010. Confidential
TEPN Internal Geological End of Well Report by Hiksdal, A., et al., 2010. D Field. Doc. Confidential
TEPN Internal Final Well A1 Report by Bourassa, K., and Grieve, C., 2003. Confidential
TEPN Internal Report by Lafont, F., Euvtard, B., 2001. Norway. Cook Sandstone of the Marflo Ridge: Nature and Distribution of the Reservoirs. Doc. No.: DGEP/GSRlTG/ISS/CLAS/O 1-0 16: Confidential
TEPN Internal Report by Lafont, F., and Marcheteau, E., 2015. NORWAY - Norwegian North Sea - Well B3: Sedimentary Geology Interpretation from Core and Borehole Image Log Data. Doc. No.: DGEP/EXPLO/TE/ISS/CLAS R13-09: Confidential
TEPN Internal Report by Bibonne, R., Euvrard, B., Marchereau, E., 2014. NORWAY - Norwegian North Sea - Well B1: Sedimentary Geology Interpretation from

Core and Borehole Image Log Data. Doc. No.: DGEP/EXPLO/TE/ISS/CLAS R13-09: Confidential

TEPN Internal Facimage Manual. Geolog® 7 – Paradigm™ 2011 With Epos® 4.1 Data Management.

Internet:

Norwegian Petroleum Directorate (NPD) 2015. Lithostratigraphy: Amundsen Formation. Accessed on the internet at http://factpages.npd.no/factpages/Default.aspx?culture=en on 15 January 2015.

Norwegian Petroleum Directorate (NPD) 2015. Lithostratigraphy: Burton Formation. Accessed on the internet at http://factpages.npd.no/factpages/Default.aspx?culture=en on 15 January 2015.

Norwegian Petroleum Directorate (NPD) 2015. Lithostratigraphy: Cook Formation. Accessed on the internet at http://factpages.npd.no/factpages/Default.aspx?culture=en on 15 January 2015.

Norwegian Petroleum Directorate (NPD) 2015. Lithostratigraphy: Drake Formation. Accessed on the internet at http://factpages.npd.no/factpages/Default.aspx?culture=en on 15 January 2015.

Norwegian Petroleum Directorate (NPD) 2015. Lithostratigraphy: Dunlin Group. Accessed on the internet at http://factpages.npd.no/factpages/Default.aspx?culture=en on 15 January 2015.

Norwegian Petroleum Directorate (NPD) 2015. Field: Knarr. Accessed on the internet at http://factpages.npd.no/factpages/Default.aspx?culture=en on 10 February 2015.

Norwegian Petroleum Directorate (NPD) 2015. Wellbore: Exploration: All. Accessed on the internet at http://factpages.npd.no/factpages/Default.aspx?culture=en on 15 March 2015.